Application of markers of genomic instability for evaluation of mutagenic effects in human cells

R.M. Aroutiounian[1], G.G.Hovhannisyan[1], N. S. Babayan [1,2],

A.T. Manukyan [2], A.A. Sargsyan[1], B.A. Grigoryan [3],

T. Liehr[4], A.N. Osipov[5,6], N.Y. Vorobyova[5,6],

T.A. Harutyunyan[1]

[1] Research Institute of Biology, Yerevan State University, 0025, Yerevan, Armenia
[2] Institute of Molecular Biology of NAS RA, 0014, Yerevan, Armenia
[3] CANDLE Synchrotron Research Institute, 0040, Yerevan, Armenia
[4] Institute of Human Genetics, Jena University Hospital, Friedrich Schiller University, 07747, Jena, Germany
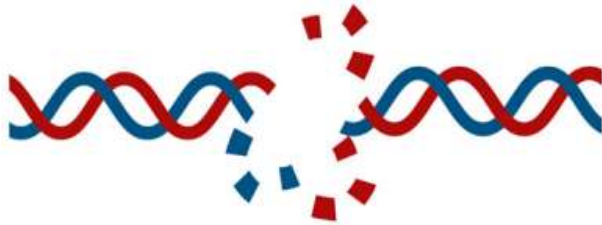[5] A.I. Burnazyan Federal Medical Biophysical Center, Moscow, Russia
[6] N.N. Semenov Federal Research Center for Chemical Physics, Moscow, Russia
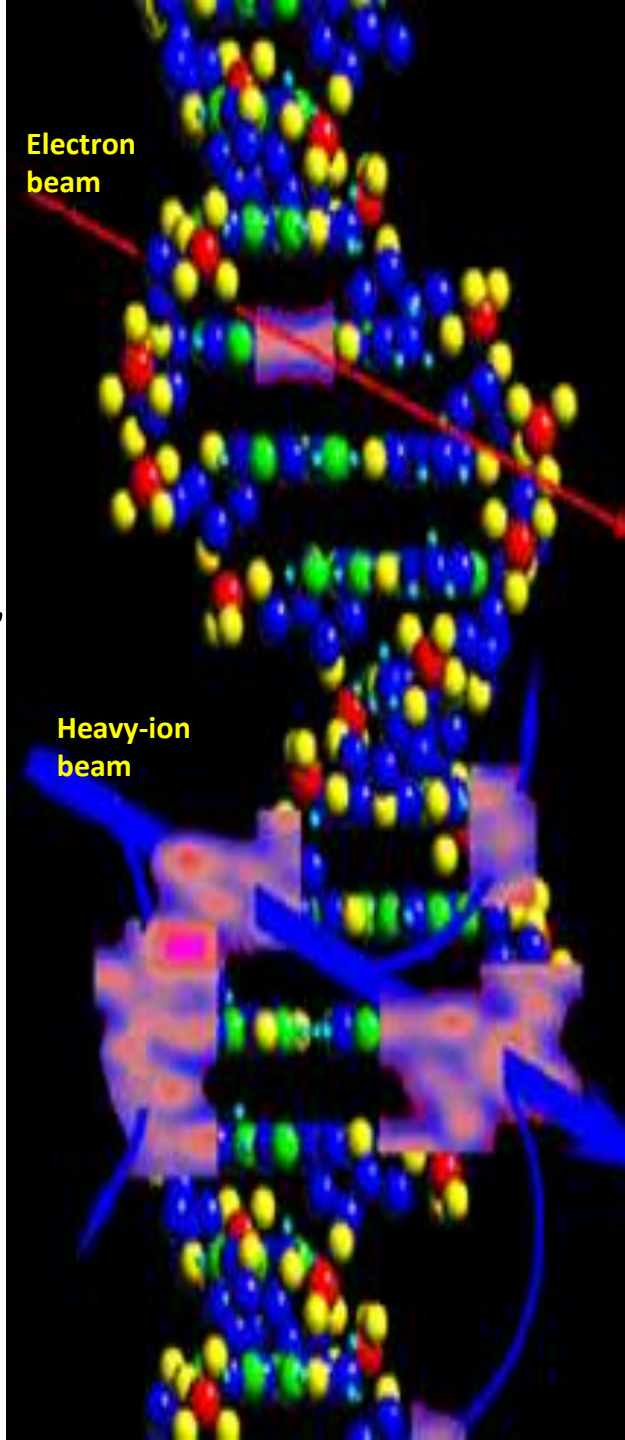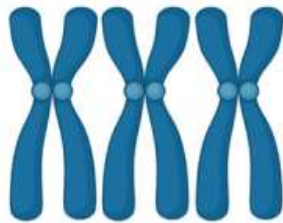
Genomic instability in cytogenetics
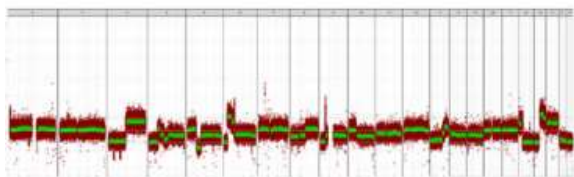
Single nucleotide variation

Double stranded breaks

Single strand breaks

Numeric chromosomal instability

Copy number alterations

GI is present in almost all tissues of the human body, and is of great importance. As the result each cell has its own genome.

GI is the result of various mutational processes occurring within the genome, ranging from single nucleotide variations, to single- or double-stranded breaks, which can lead to large and small structural changes, respectively to the chromosomes.

Numerical instability, through whole-chromosome or genome duplication, may be the result of earlier mutations, such as tumor-suppressor gene alterations.
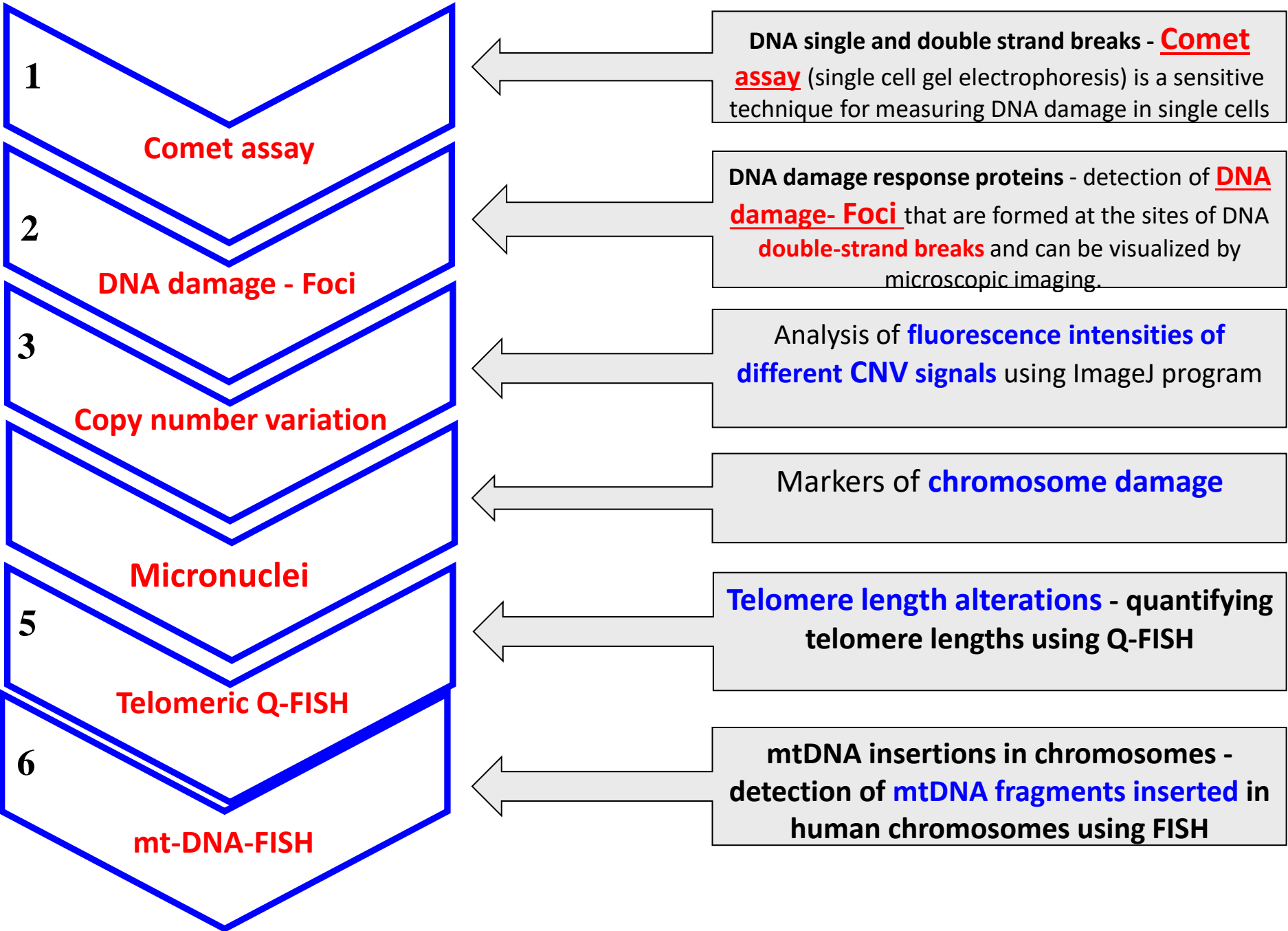
Copy number variation, which result in gains or losses of genomic segments, can drive further instability and may help provide early diagnostic information.
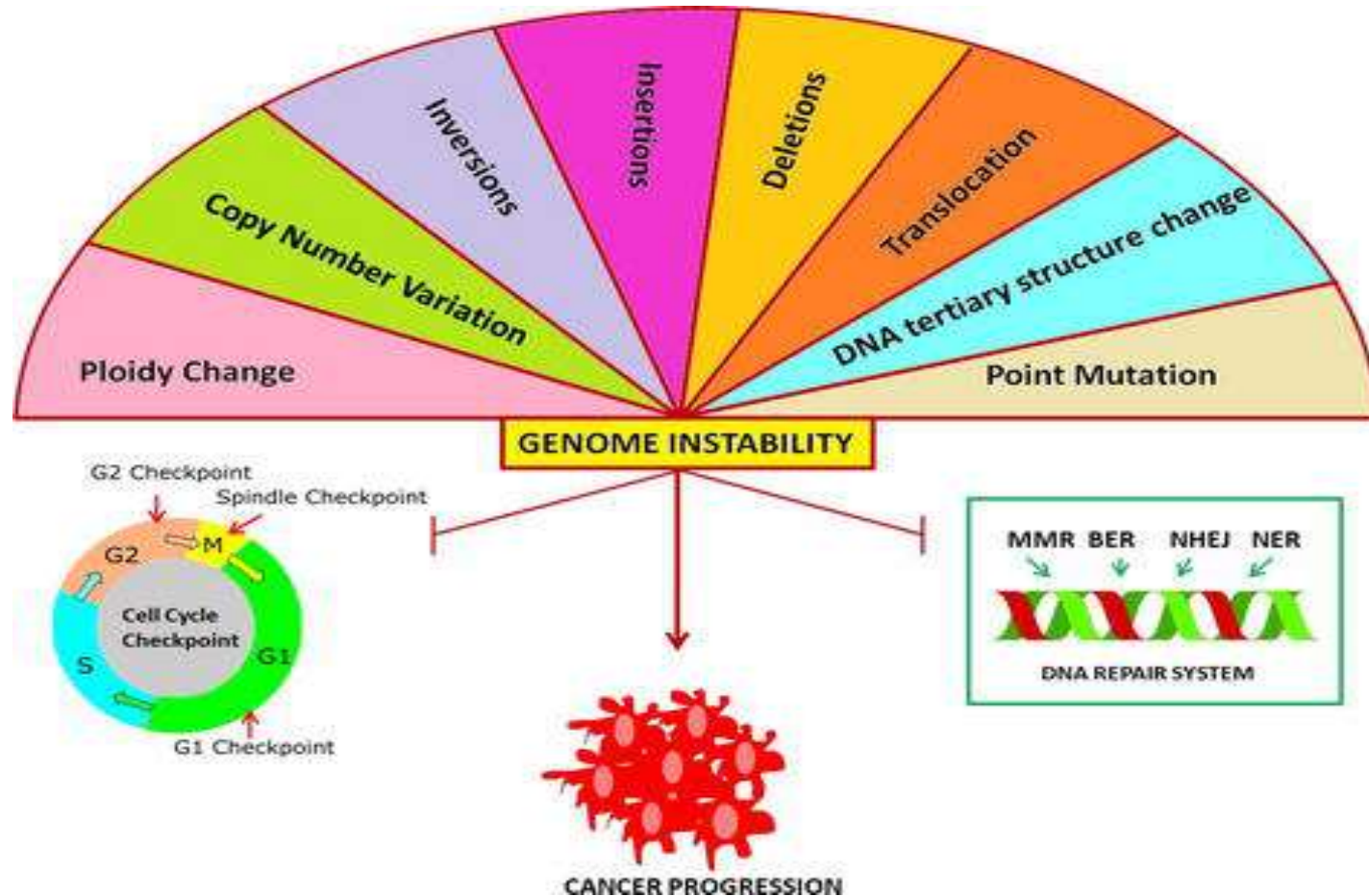
Killcoyne et al. *Trends Genet*. 2021;37(11):966-972.

Barbara McClintock

Nobel Prize Geneticist
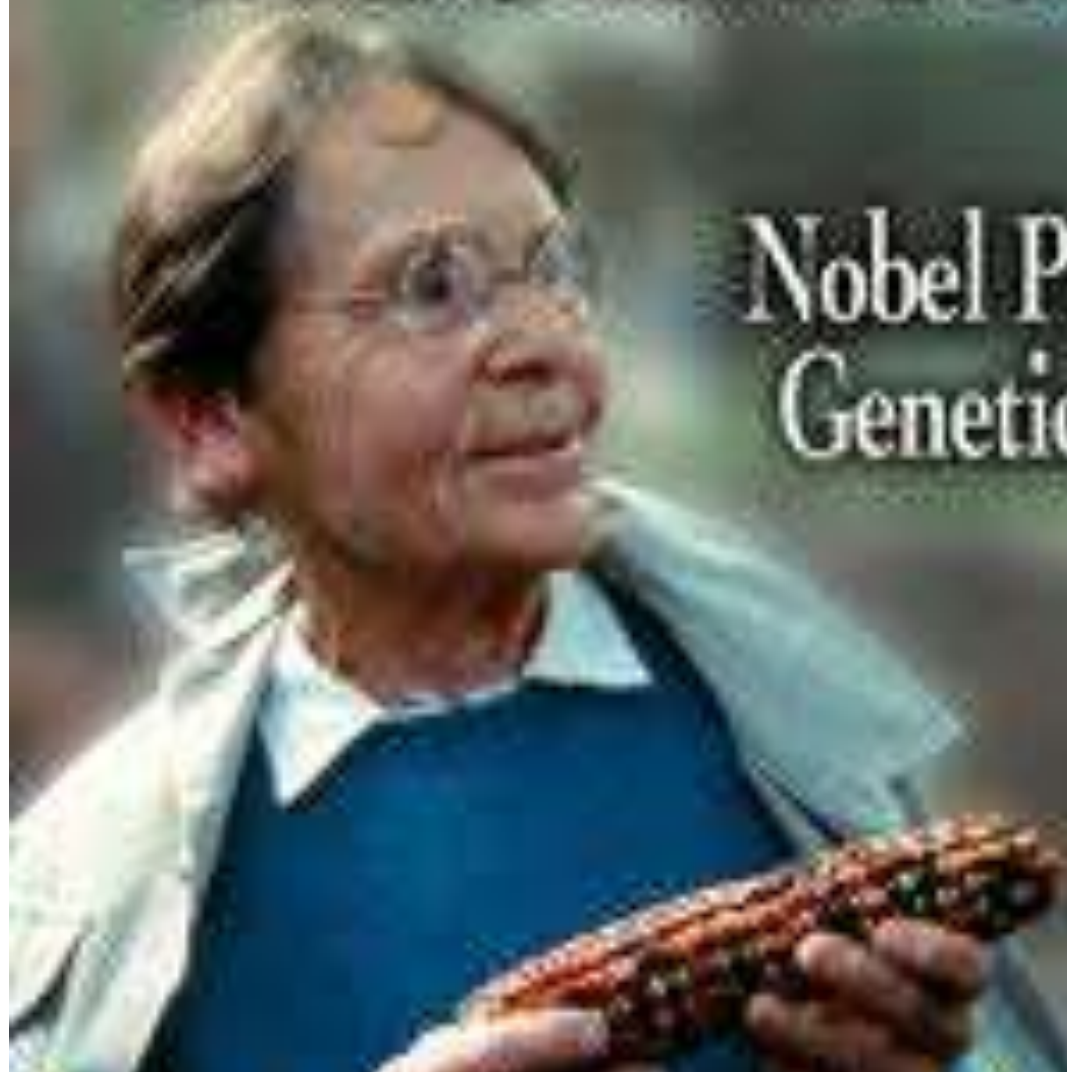
For evaluation of of genomic instability in human cells we apply the following markers of mutagenic effects :

1 — **Comet assay**

DNA single and double strand breaks - **Comet assay** (single cell gel electrophoresis) is a sensitive technique for measuring DNA damage in single cells

2 — **DNA damage - Foci**

DNA damage response proteins - detection of **DNA damage- Foci** that are formed at the sites of DNA **double-strand breaks** and can be visualized by microscopic imaging.

3 — **Copy number variation**

Analysis of **fluorescence intensities of different CNV signals** using ImageJ program

4 — **Micronuclei**

Markers of **chromosome damage**

5 — **Telomeric Q-FISH**

Telomere length alterations - quantifying telomere lengths using Q-FISH

6 — **mt-DNA-FISH**

mtDNA insertions in chromosomes - detection of **mtDNA fragments inserted** in human chromosomes using FISH

Genomic instability influencing cancer.

There are several type of repair pathways namely: nucleotide excision repair (NER), base excision repair (BER), DNA mismatch repair (MMR) and double strand break repair which includes homologous recombination (HR) and non-homologous end joining (NHEJ). Every one of them are specialized in a specific type of repair pathway

- **About 50 % of cancer cases are treated with radiation therapies (possibly in combination with surgery and/or chemotherapy).**

- **Among these treatments, more than 50 % use RF-driven linear accelerators of electrons (RF-Linac).**

- **Other techniques include internal radiation (brachytherapy) and proton-ion beams (hadrotherapy).** In most cases electrons delivered by a RF-linac are not used directly on the tumor, but converted into photons (**hard X-rays**) by bremsstrahlung through a suitable target.

- **Electrons are used directly, either to cure superficial tumors or in the Intra-Operative Radiation Therapy**

AREAL

laser driven linear accelerator providing ultrashort electron pulses

(sub-pico or femtosecond) with the electron energy in MeV domain

- pulse duration - **0.04x10^{-12} s**
- UHPDR - **1.6x10^{10} Gy/sec**

> JETI and ELBE
> ~ **1-5x10^{-12} s**
> ~**10^8-10^9 Gy/sec**

AREAL produces electron pulses generated by UV laser and accelerated using high gradient RF resonator

The advantage of laser-generated ultrafast electron beams for biological and clinical application:

-Typically feature a monoenergetic spectral profile and are better directed (less lateral spread) than other laser-driven ions.

-Areal is important for biologists due to very high instantaneous dose delivery within a time interval shorter (sub-pc vs. pc), than many chemical reactions, pulses of enormous capacity (10^{10} Gy/sec vs. 10^8-10^9 Gy/sec).

-This allows the precise dose-control induction of local effects on cells and solid tumors **with minimal exposure of normal tissues.**
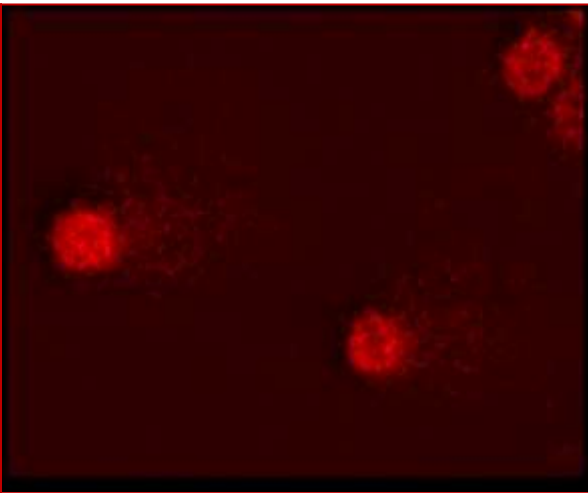
Comet assay

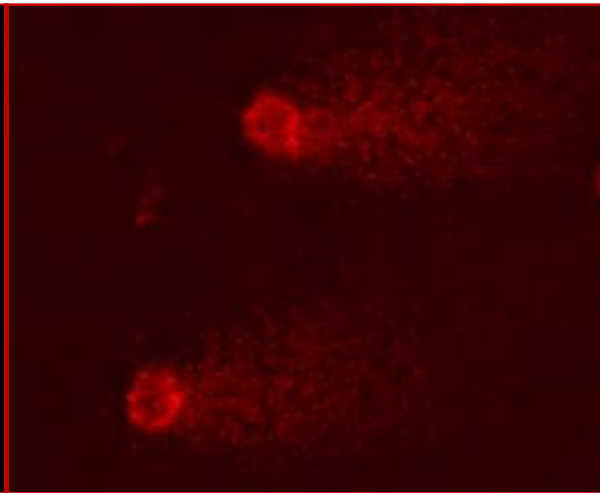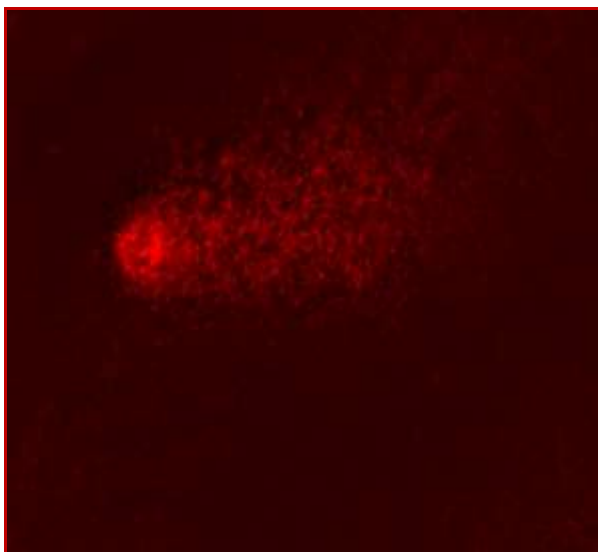Analysis of DNA damage using comet assay –single cells electrophoresis
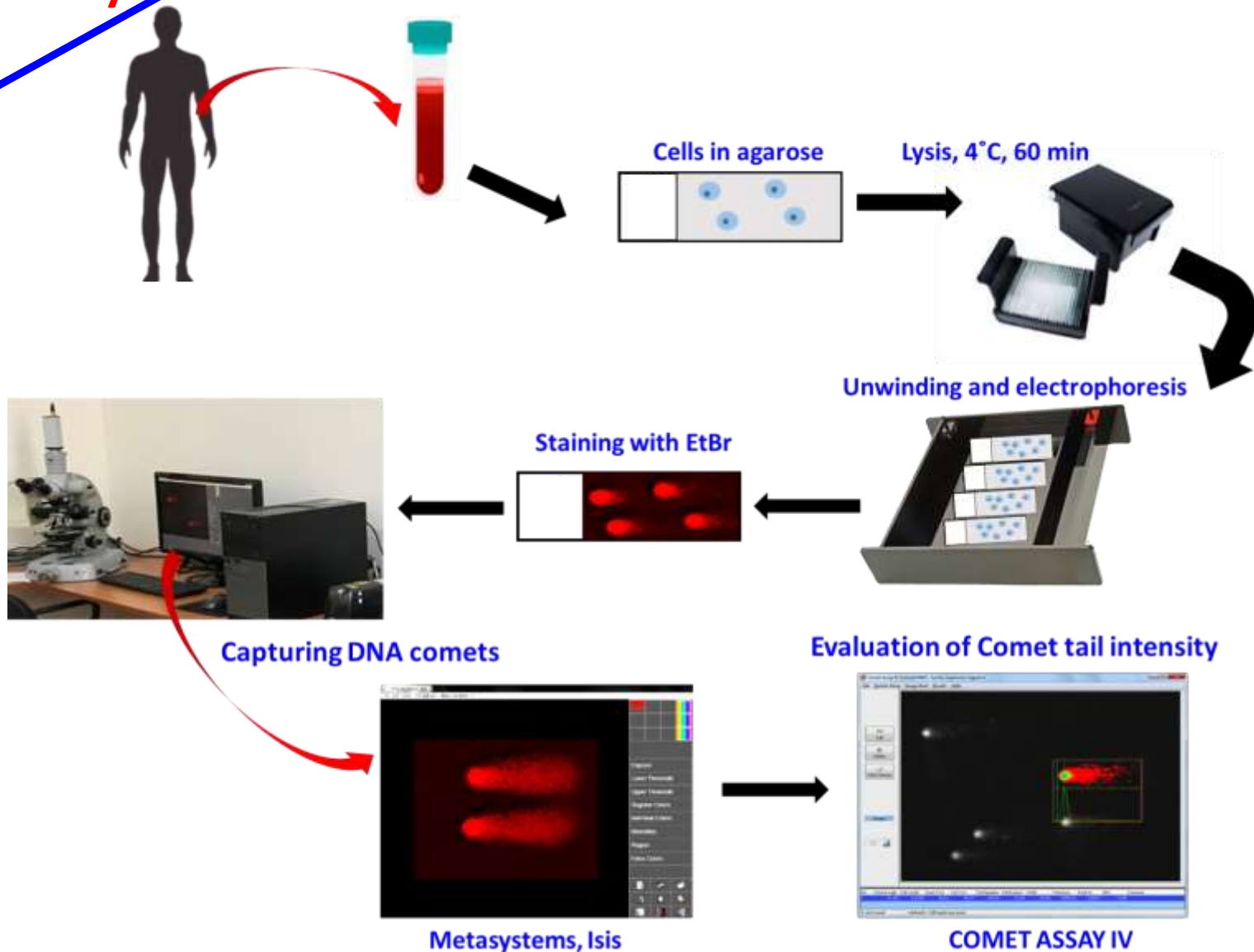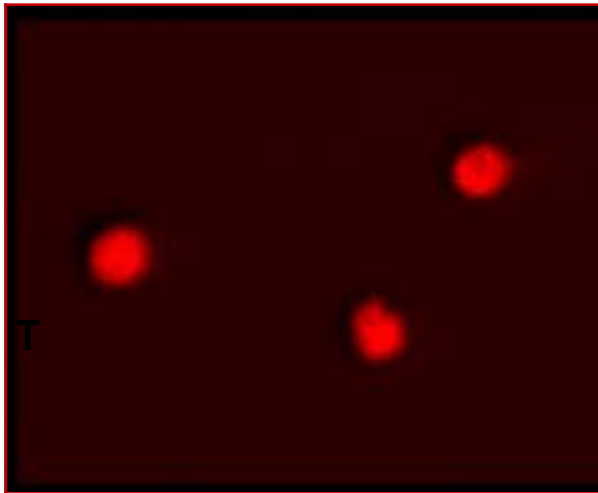
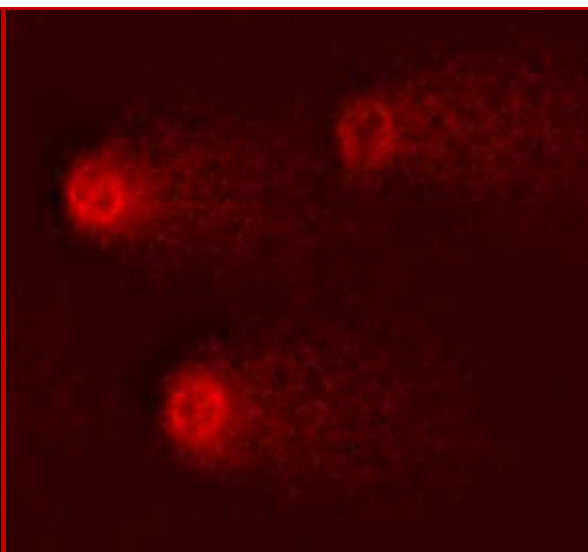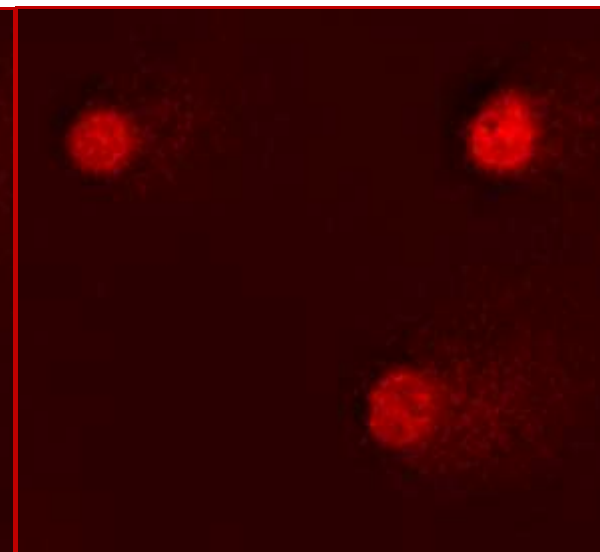**Non-irradiated control**   **Irradiation, dose 2 Gy**   **Irradiation, dose 4 Gy**

Irradiation, dose 8 Gy   **Irradiation, dose 16 Gy**   **Irradiation, dose 24 Gy**
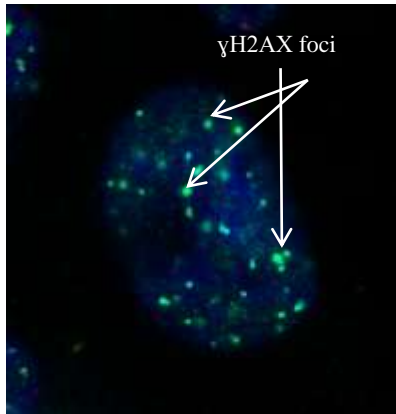
Comet assay images of K-562 (human chronic myelogenic leukaemia) cells after irradiation by AREAL

DNA damage foci

DNA damage FOCI are **distinct spots** consisting of **DNA damage repair proteins** that occur **in DNA double strand breaks (DSBs) loci.**

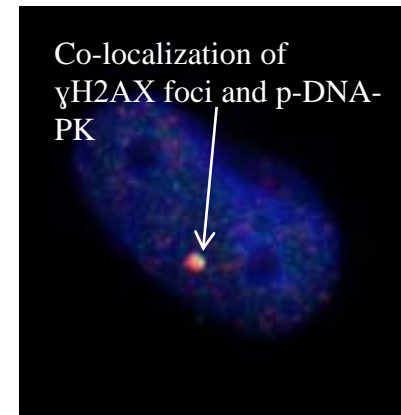**FOCI contain hundreds to thousands of copies of various proteins involved in DNA DSB repair.**

γH2AX foci

Visualization of phosphorylated γH2AX foci in irradiated cell

Fluorophores

γH2AX foci – Fluorescein (FITC) – green

p-DNA-PK - Texas Red - red

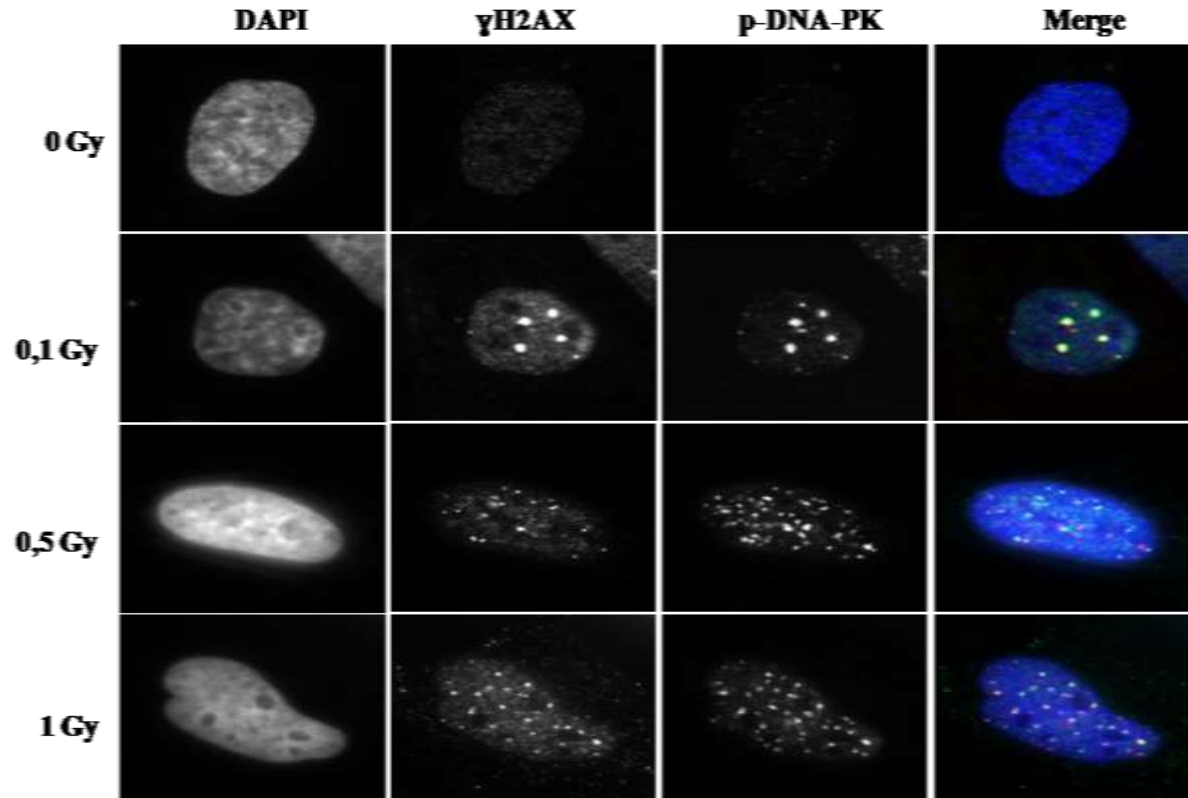
Co-localization of γH2AX foci and p-DNA-PK

Co-localization of phosphorylated γH2AX and DNA-PK protein can be visualized

One of the earliest (several minutes) DNA repair events is the phosphorylation of a protein called histone H2AX, that involves many other proteins in the repair process, which are sensors of DSBs (For low-LET we measured DNA-PK).

The quantitative analysis of the foci of repair proteins and their localization in the post-radiation period **allows to determine not only the number of DSBs and their spatial distribution in the cell nucleus, but also the mechanisms of their repair.**

Co-localization of γH2AX foci and p-DNA-PK at different doses of AREAL irradiation

The ultrashort electron beam radiation effect on DNA DSBs formation

The γH2AX and p-DNA-PK foci and their co-localization
at 1h post-irradiation in human fibroblasts

Energy vs. time emitted from a laser

a) typical **continuous wave (CW) laser**; constant energy over time.
b) **CW laser quasi-continuous irradiation**; average power is reduced but no gain in peak power.
c) **Ultrashort pulse laser**; average power remains the same but peak power is greatly enhanced.
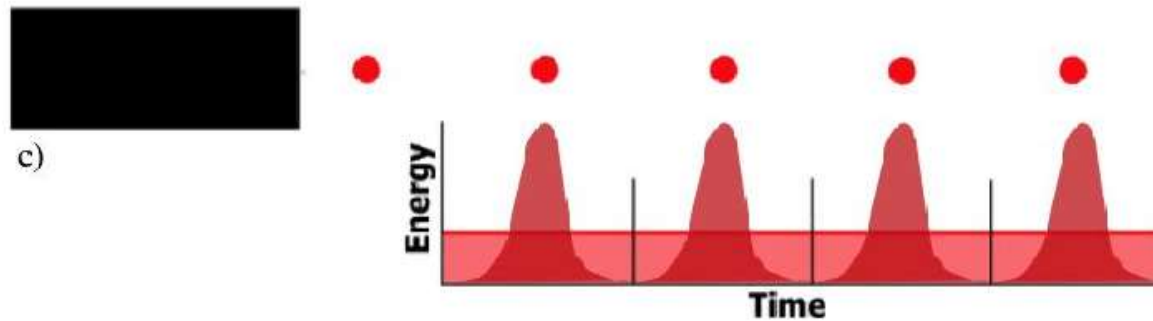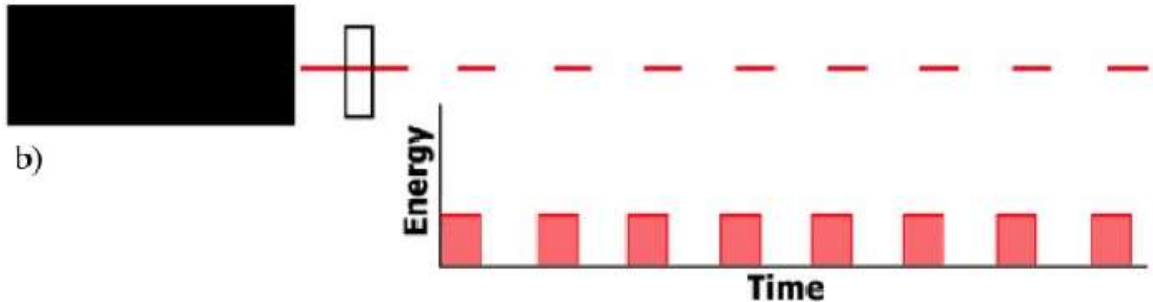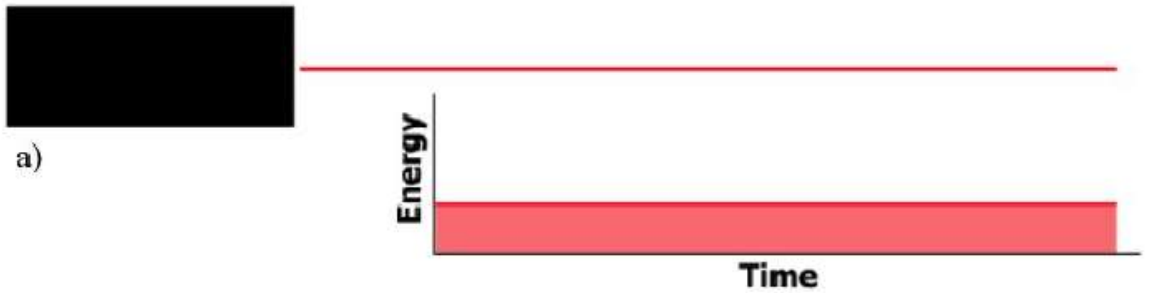
Comparative studies of radiobiological effects for AREAL and Varian accelerators

Varian Trilogy linear electron accelerator (Varian Medical Systems, USA)

- For **quasi-continuous irradiation**, a Varian Trilogy linear electron accelerator (Varian Medical Systems, USA) was used.

- Characteristics: electron energy - 4 MeV, dose-rate 5.6 Gy/min, electron beam spot 250×250 mm.

- Dosimetry was carried out by the ionization chamber method of absorbed dose measurement in the water phantom according to the international protocol IAEA TRS-398.

AREAL *vs* Varian

Dose-dependent changes in the γH2AX residual foci numbers in HeLa and A549 both **lung carcinoma cells** at 24 h post-irradiation
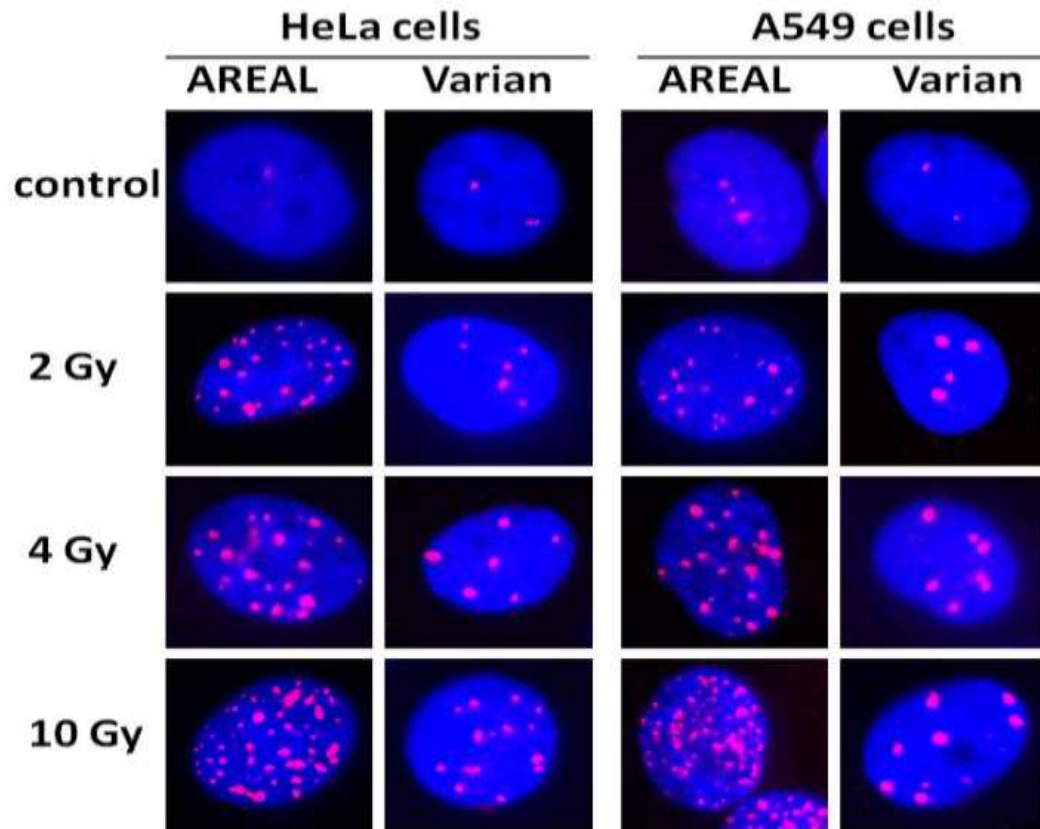

- **For AREAL irradiation is demonstrated slower DSB repair rate induced by ultrashort pulsed irradiation for both cell types , compared to Varian.**
- **Why? Pulse duration increases the possibility of DSB-complex with more difficulty repairable DSBs formation.**
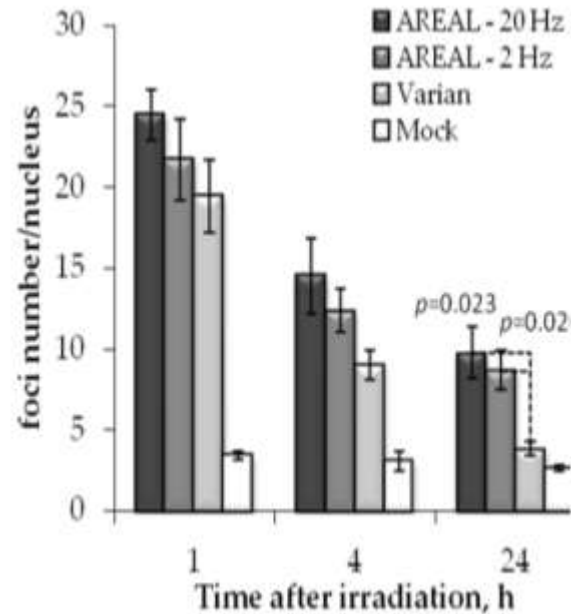
AREAL *vs* Varian

Post-irradiation changes of the γH2AX and 53BP1 FOCI (markers for DNA DSBs) in HeLa cells, irradiated on AREAL and Varian accelerators at a 1 Gy dose
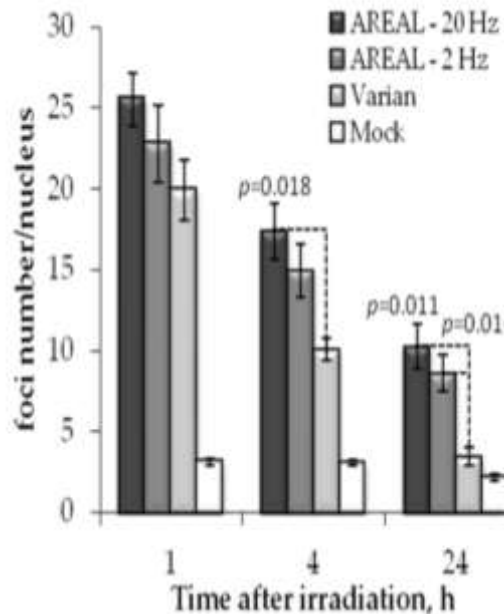
γH2AX FOCI   **53BP1 FOCI**

1. No significant difference between the effects of pulsed irradiation at 2 and 20 Hz
2. 24 h post-irradiation, the significant difference between the effects of pulsed and quasi-continuous irradiations was observed at both pulse rates (2 and 20 Hz)
3. 24 h after exposure to pulsed irradiation, the foci number for AREAL was 2.5–2.9 times higher as compared with Varian. Similar trends were observed also for 53BPI foci.

Pulsed irradiation induces more difficultly repairable complex DSBs

Tumor protein P53, is cellular tumor antigen the "Guardian of the Genome"

*p53-binding protein 1 (**53BP1**) is a crucial component of*
***DNA double-strand break signalling** and **repair activator** in mammalian cells*
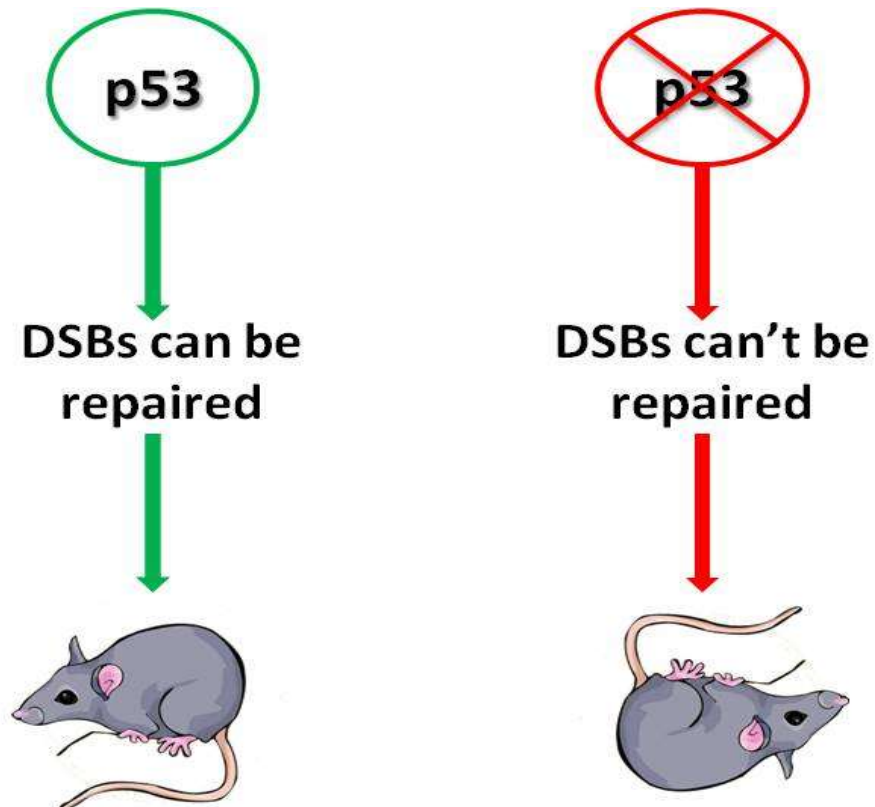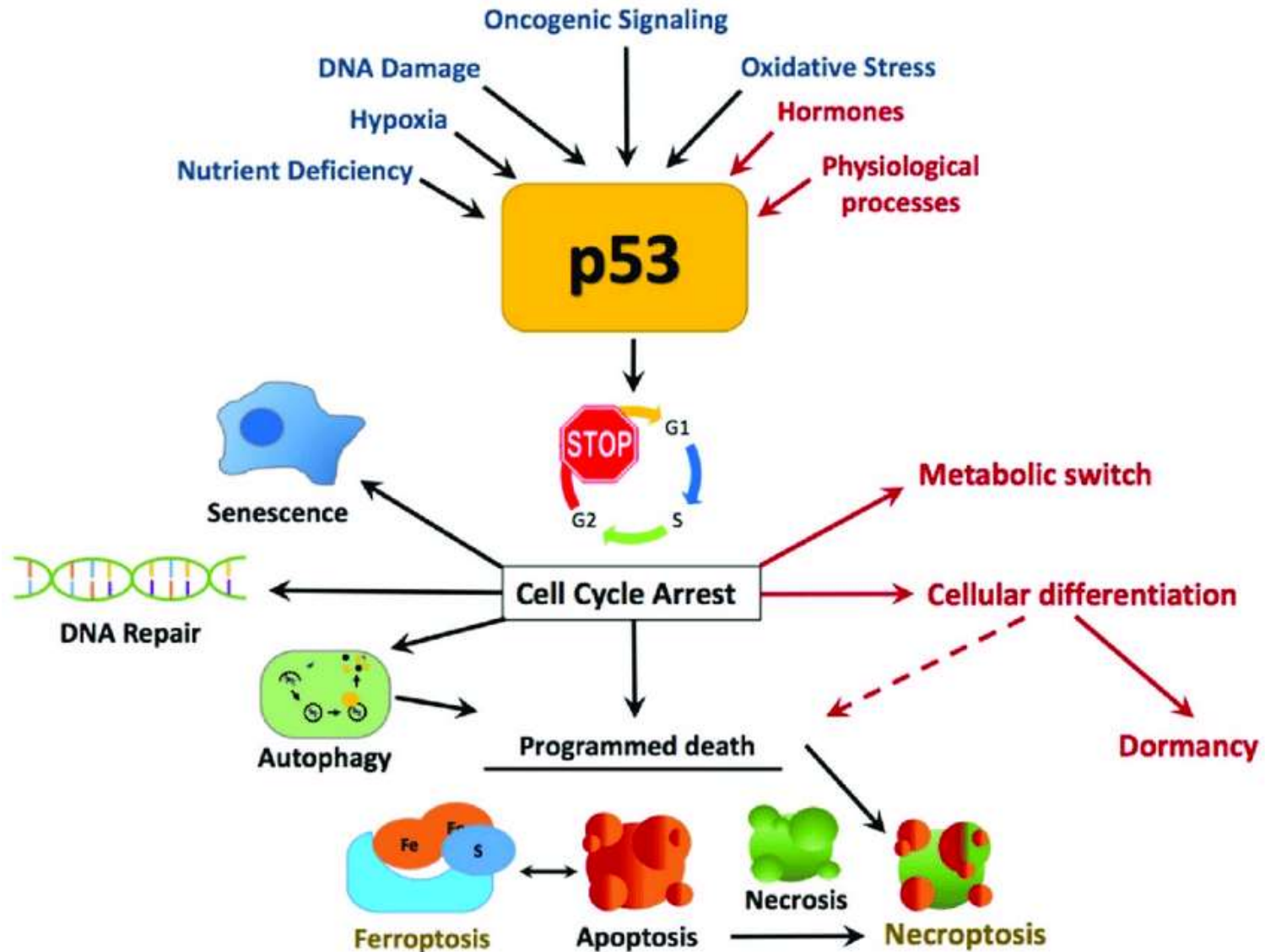
The biological role of p53 –
that arrests cell cycle until repairing DSBs

AREAL vs Varian

Residual γH2AX Foci in A649 and H1299 (p53-deficient Human Lung Carcinoma Cells) Exposed to Subpicosecond Beams of Accelerated Electrons

A549 (p53 wild type cells)
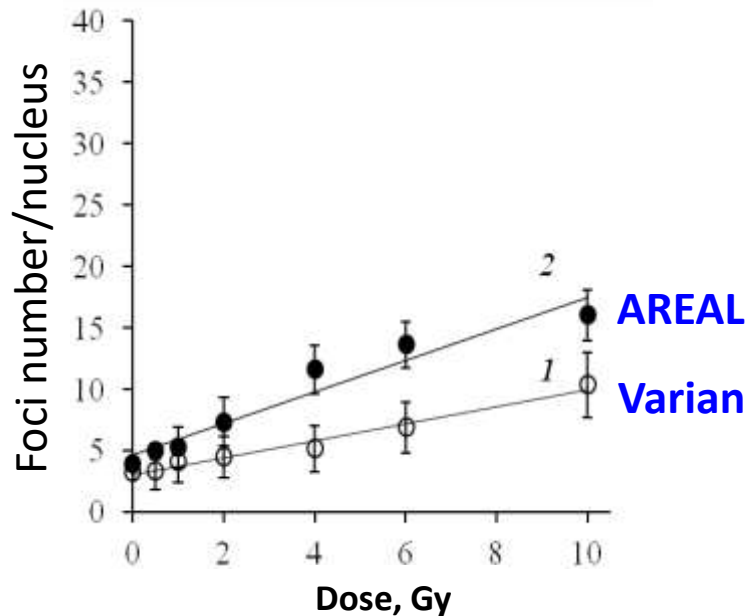
H1299 (p53-deficient)
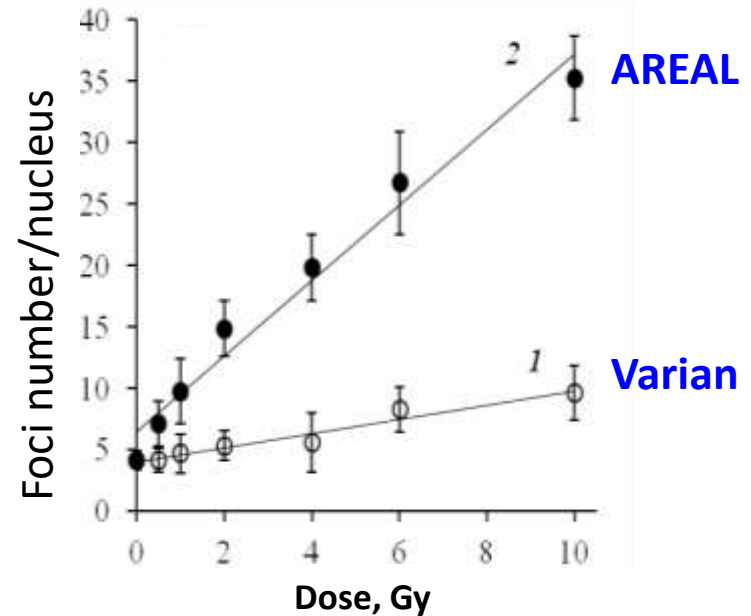
Comparison of the slope coefficients showed that yield of γH2AX foci exposure was

Foci for AREAL 1.8 times (DSB-complex), than for Varian in A549, and 5.3 times higher in H1299 .

H1299>A549 (more FOCI), especially for Areal, because of

weakened repair for Areal in the absence of p53, due to complex damages.

Conclusion: the yield of FOCI in human cells is p53-dependent for AREAL irradiation, but not for Varian!

Micronuclei

The induction of chromosomal aberrations, such as <u>chromosomal fragments resulting from DNA breaks, or entire chromosome loss</u> was evaluated in MRC5 cell line after 0.1 Gy, 0.5 Gy and 1 Gy doses of electrons and X-ray irradiation.

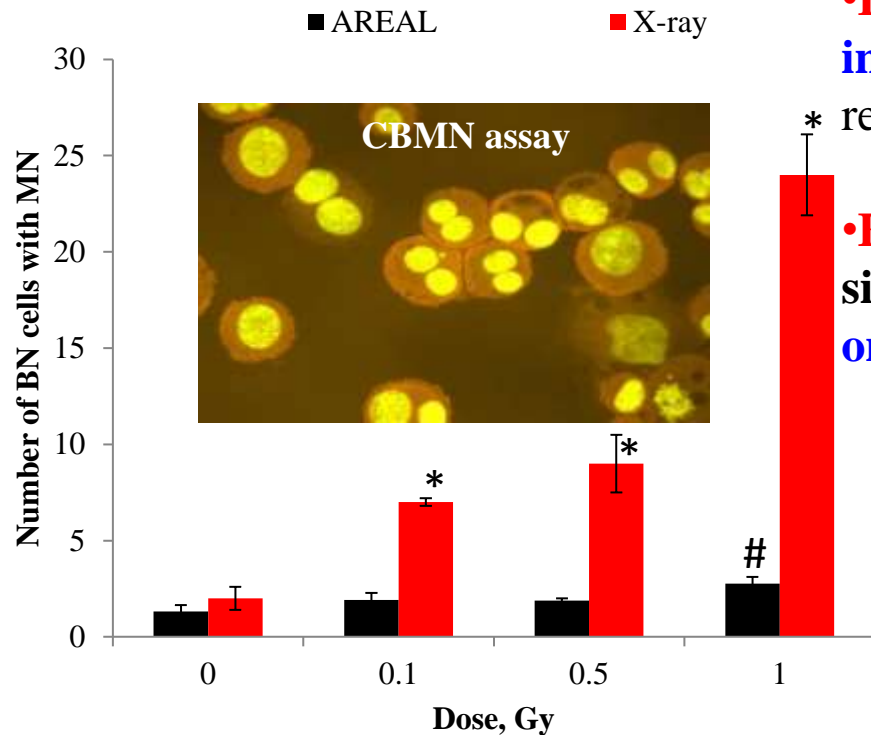•**For X-ray irradiation the dose-dependent increase of MN frequency was observed**, reaching the level of 24±2.1 of BN cells with MN

•**For AREAL the slight, but statistically significant increase was observed only at the 1 Gy of electrons irradiation**

RBE (relative biological effectiveness) value was calculated as the ratio of the <u>**slopes**</u> for the two radiation types
**The dose-response functions were**
•AREAL y=<u>**1.1979**</u>x+1.4864 (R^2=0.83)
•X-ray y=<u>**20**</u>x+2.5 (R^2 = 0.92)

The deduced RBE value of AREAL iradiation to **X-rays** to induce micronuclei in **MRC5 cells** was about **0.06. Lower level of MN in case of electrons iradiation was due to death of cells, not aberrations transmission in generations!**

Results of transcriptomics analysis of DNA Repair Pathway Activation Levels
of wild-type **A549** and p53-deficient **H1299** human lung carcinoma cells

DNA Repair Pathways
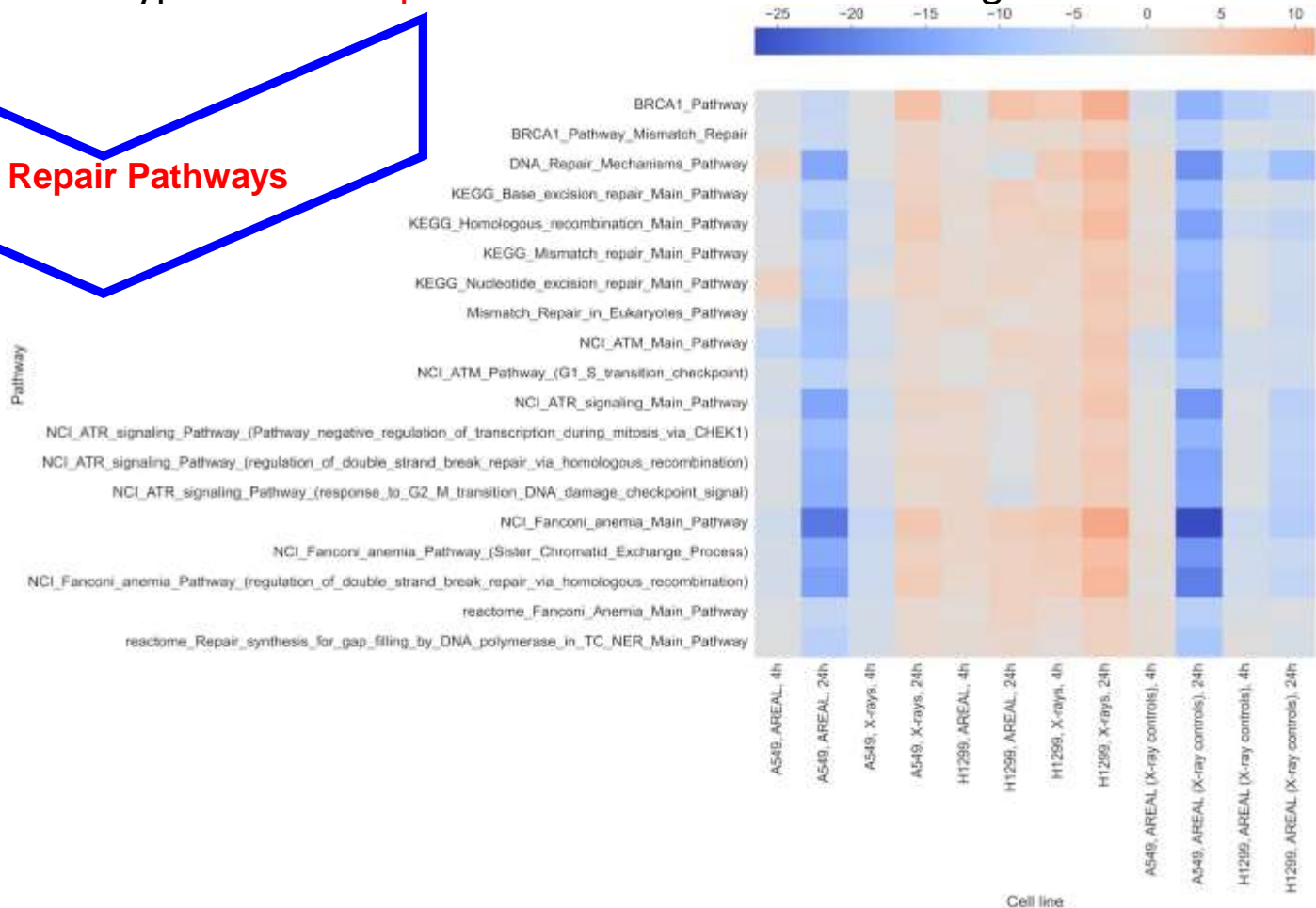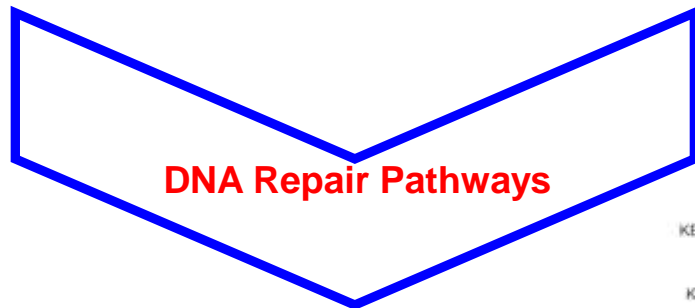
AREAL vs X-rays The gene expression analysis of 19 DNA **repair** pathways had shown:
both AREAL (5) and **X-rays-exposed H1299 (7) cells with slight increase in DNA repair PALs** compared to **more pronounced !!! increase in DNA repair activity by 24 hours after X-rays exposure (8).**

Was revealed **strong p53-dependent action** of **AREAL** irradiation differs from X-rays(column 10):
down-regulation of DNA repair in H1299 cells (columns 11 and 12) 4 and 24 hours after irradiation.

Conclusions 1

1 **Ultrashort pulsed AREAL radiation, which causes DNA damage**, is characterized by a **slow rate of DSB repair**. Apparently, this **increases the probability of the formation of complex and difficult to repair DSBs.**

2. **The radiosensitivity of cells to AREAL irradiation is p53-dependent**. p53-deficient (the most common cancer cells) are more sensitive to AREAL irradiation.
Since p53 is a tumor suppressor protein, **this advantage of AREAL radiation can be used in the future to ensure the specificity of cancer cells during irradiation**, which will reduce the side effects associated with damage occurring in normal cells.

3. Radiation-induced cytogenetic abnormalities such as micronuclei formation are an early marker of possible delayed effects. **These delayed effects may lead to secondary cancers when the body is irradiated.** Our study shows a significantly lower frequency of micronuclei with AREAL irradiation compared to X-rays.

4.**The formed and unreparable γ-H2AX foci by Areal lead to apoptotic cell death in the absence of genomic instability at the chromosomal level.**
Thus, it can be assumed that **AREAL radiation has a lower potential to induce secondary cancers when irradiated as a whole body treatment.**

5. **AREAL irradiation is more effective in vitro compared to X-rays and quasi-continuous irradiation (Varian) used in clinical practice.**

Telomeres
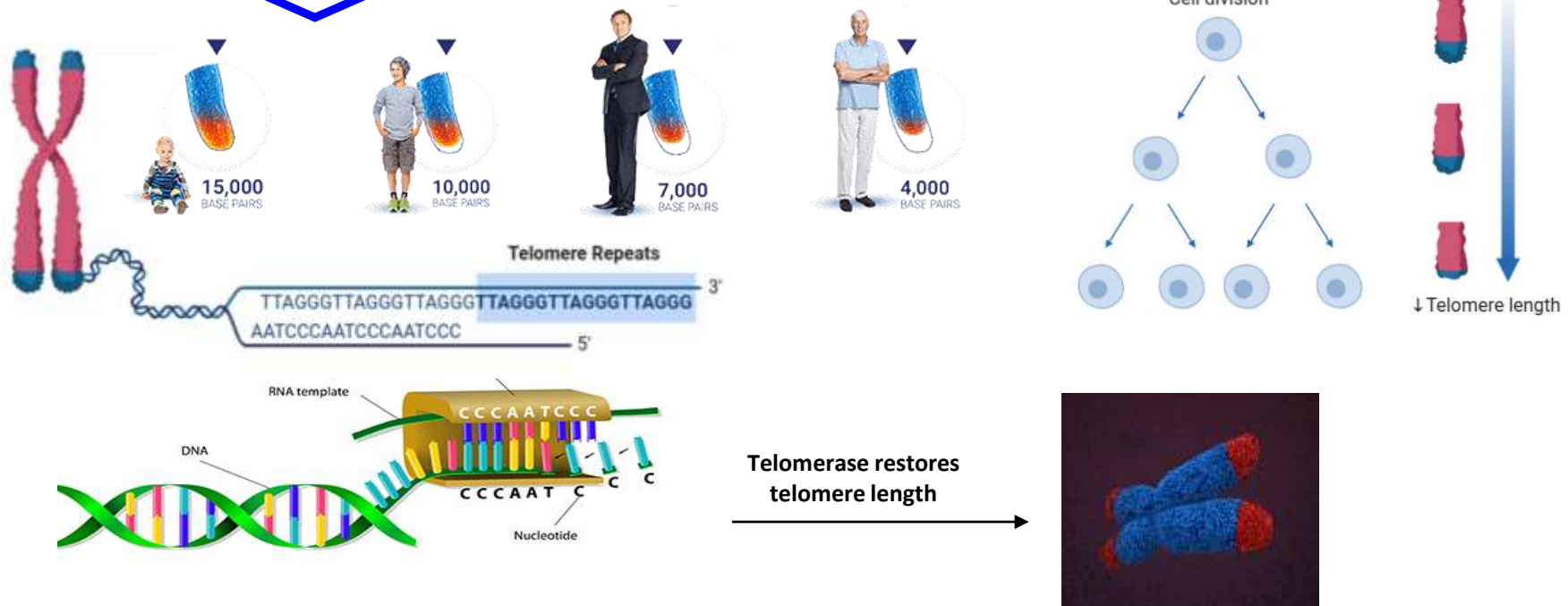
-**Telomeres are nucleoprotein structures with repeated sequences of DNA** (TTAGGG)n that cap the end of each chromosome arm and function to maintain genome stability.

-**With each cell division the length of telomeres gets shorter which limits cell divisions**. Also, telomere attrition is correlated with the process of aging.

-However, telomere length can be restored by the enzyme telomerase
 which is constantly active in cancer cells.

Therefore, a detailed understanding of the mechanisms of telomere loss and preservation is important for human health.

Telomere attrition can be induced by environmental factors

Radiation
(UV, ionizing)

Environmental factors
(smoking, air pollution,
chemical mutagens)
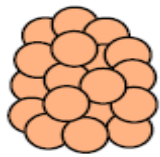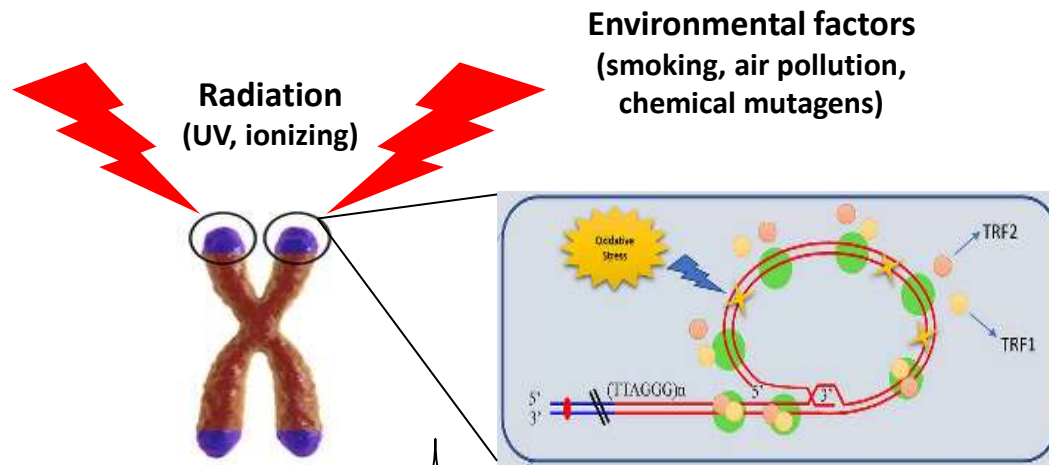
Cancer

Cellular senescence
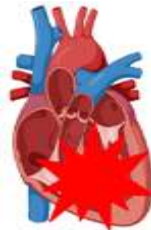
Cardiovascular diseases

Neurodegenerative and
age-related diseases

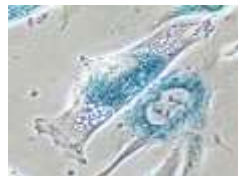-Alterations of telomere length are associated with various pathological conditions including cancer, cellular senescence, cardiovascular, autoimmune and neurodegenerative or aging-related diseases

-Environmental factors such as radiation and chemical compounds can increase telomere damage mainly via induction of DNA oxidative damage due to high concentration of G-rich parts in telomeres.

-Telomere shortening suppresses cell division by triggering senescence in normal cells and can promote cancer by triggering genomic instability.

-In recent years telomere length alterations have been used as molecular markers for the evaluation of biological effects of radiation.

However, the impact of accelerated electrons on telomere length was not studied yet.

Quantitative Fluorescence in situ hybridization or Q-FISH

Telomeres

Telomeres

Telomeric DNA

DNA denaturation and hybridization with the probe

PNA probe

Q-FISH analysis

Metaphase chromosome

Interphase nucleus
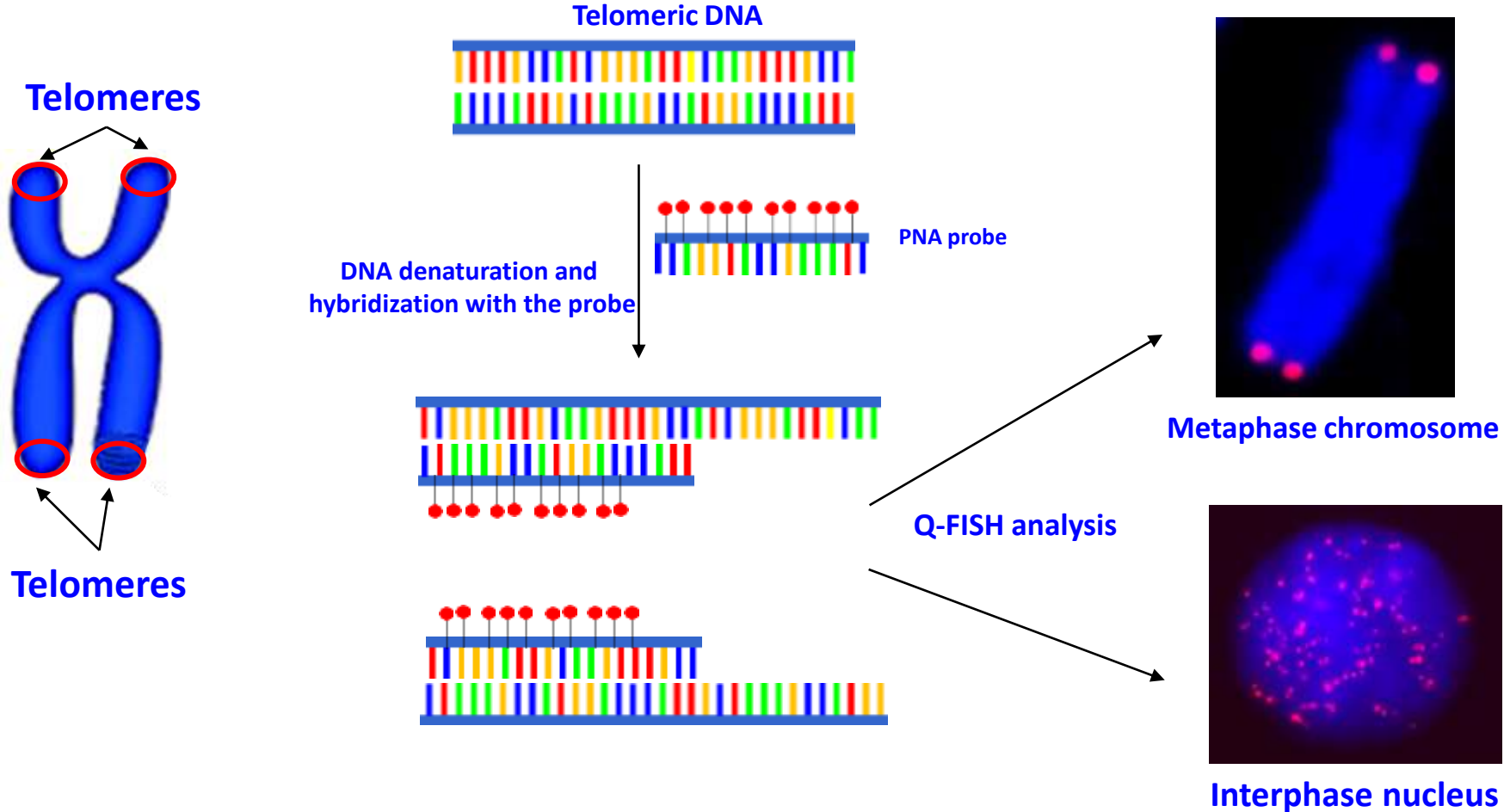
Correlations between telomere lengths and doses of AREAL electron beam in metaphases and interphases of normal blood leukocytes and interphases of K562 cells
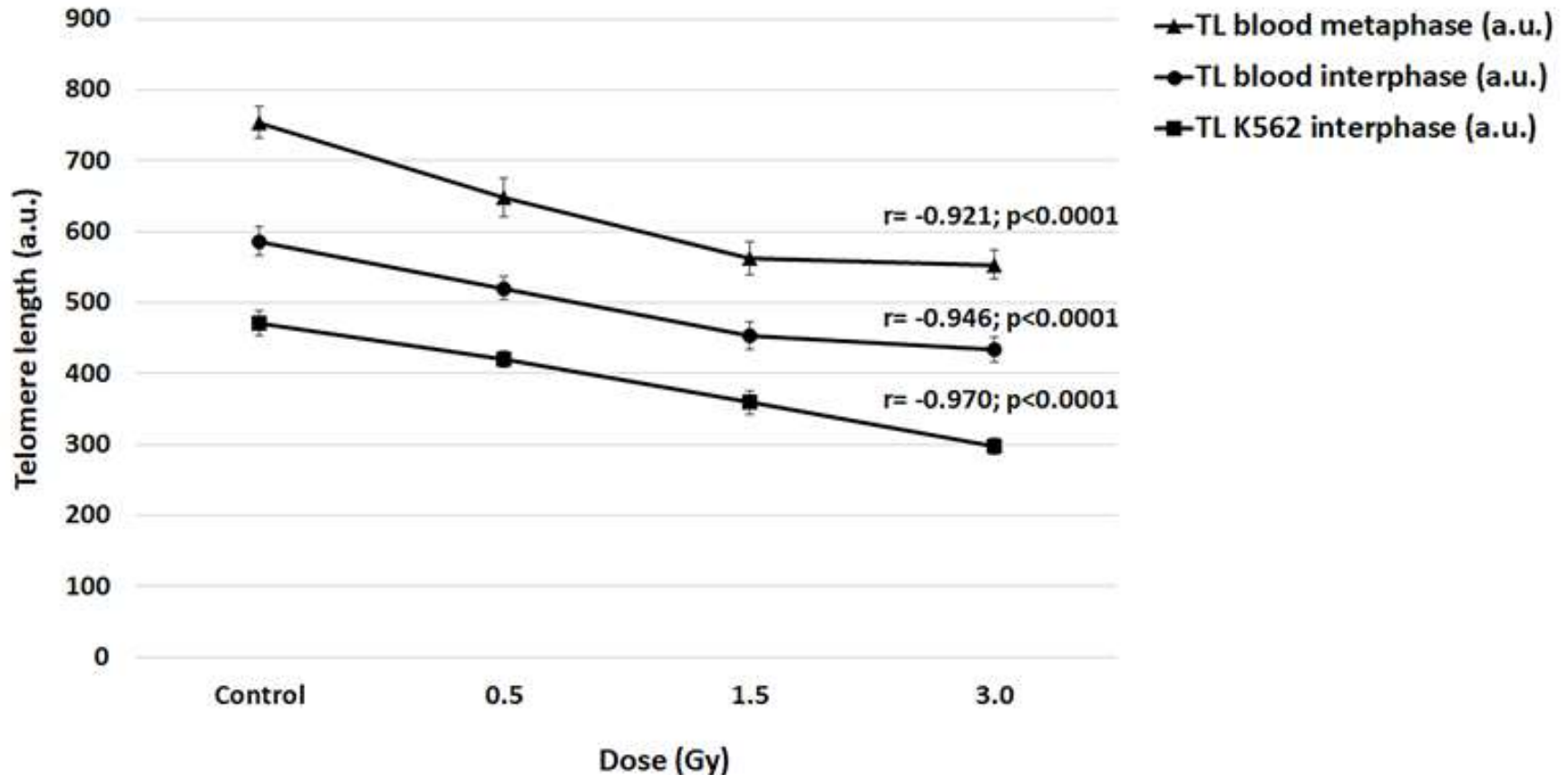
Spearman's rank correlation analysis indicates **dose-dependent telomere shortening** both in **metaphase** chromosomes ($r = -0.921$; $p < 0.0001$) and **interphase nuclei** ($r = -0.946$; $p < 0.001$) **of blood leukocytes** and in **interphase nuclei of K562 cells** ($r = -0.970$; $p < 0.0001$)

Changes in Telomere Length in Leukocytes and Leukemic Cells after Ultrashort Electron Beam Radiation

Tigran Harutyunyan, Anzhela Sargsyan, Lily Kalashyan, Hovhannes Igityan, Bagrat Grigoryan, Hakob Davtyan, Rouben Aroutiounian, Thomas Liehr , and Galina Hovhannisyan

The percentage of telomeres, shorter than the 20th percentile of the control variant in blood and K562 cells irradiated with different doses of laser-generated electron beam

Cells (20th percentile of control)	0.5 Gy (%)	1.5 Gy (%)	3.0 Gy (%)
Blood metaphases (640.40 a.u.)	47.50	79.17	81.67
Blood interphases (462.48 a.u.)	22.70	55.97	63.41
K562 interphases (363.01 a.u.)	23.17	55.49	79.88

Kolmogorov–Smirnov test revealed statistically significant differences between the distributions of TLs in irradiated and control blood and K562 cells.

Thus, an increase in the proportion of the shortest telomeres with increasing radiation doses in all experimental variants was detected.

Copy number variation - CNV

Deletion ← **Duplication** →
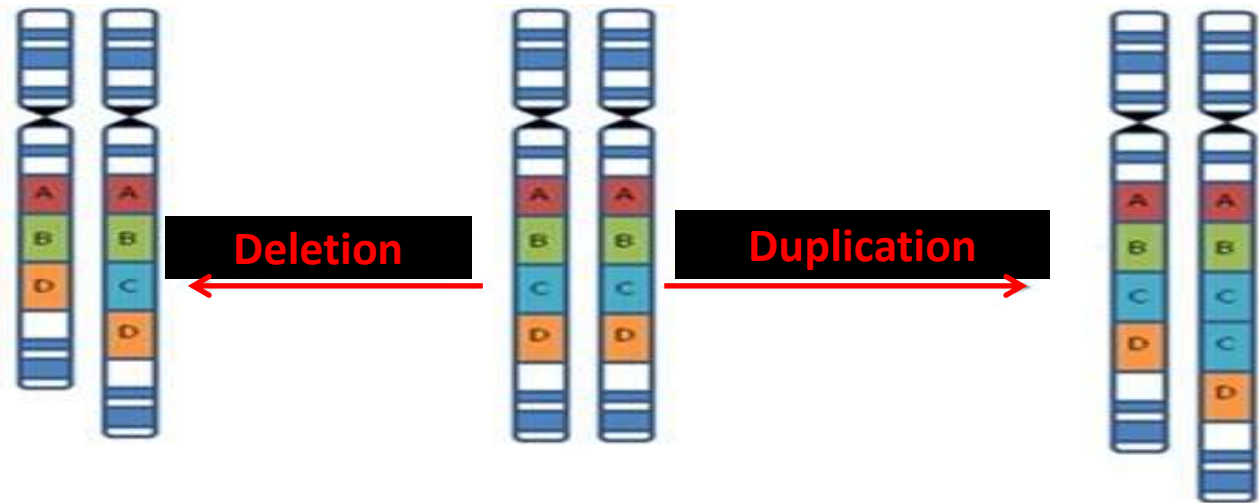
CNVs are sequences of DNA of 50 bp or larger compared with its reference genome, up to 9.5 % of the human genome contributes to spontaneous CNVs.

CNVs are now recognized as one of the major sources of genetic variation. Despite their importance little is known about environmental risk factors affecting CNVs.

De novo CNVs can arise after influence of replication inhibitors (aphidicolin, hydroxyurea, ionizing radiation), these findings have been confirmed by our group.
We studied induced CNVs with application of chemical and physical mutagens.

Analysis of fluorescence intensities using Scion Image - different sizes of probes signals
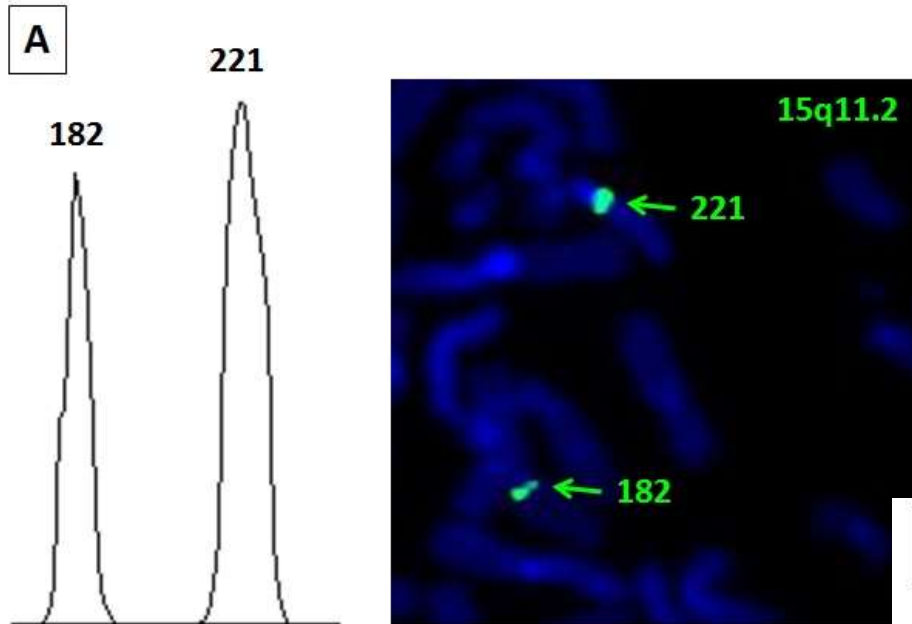
Fluorescence intensities of CNVs on homologous chromosomes 15q11.2

Fluorescence intensities of CNVs on homologous chromosomes 8p21.2

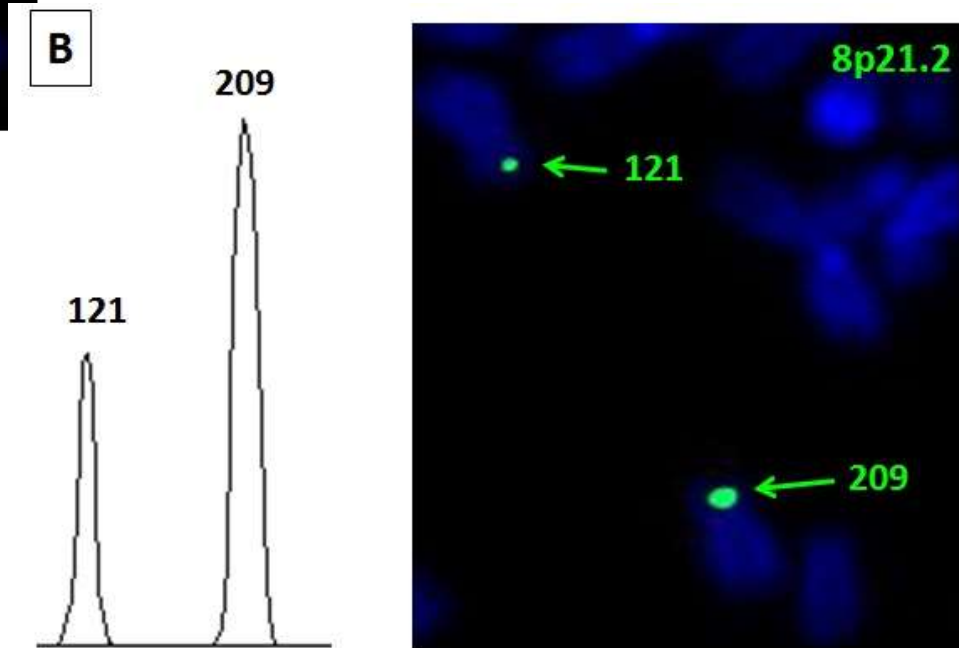# Analysis of CNVs induced by ultrashort electron beam radiation in human leukocytes in vitro
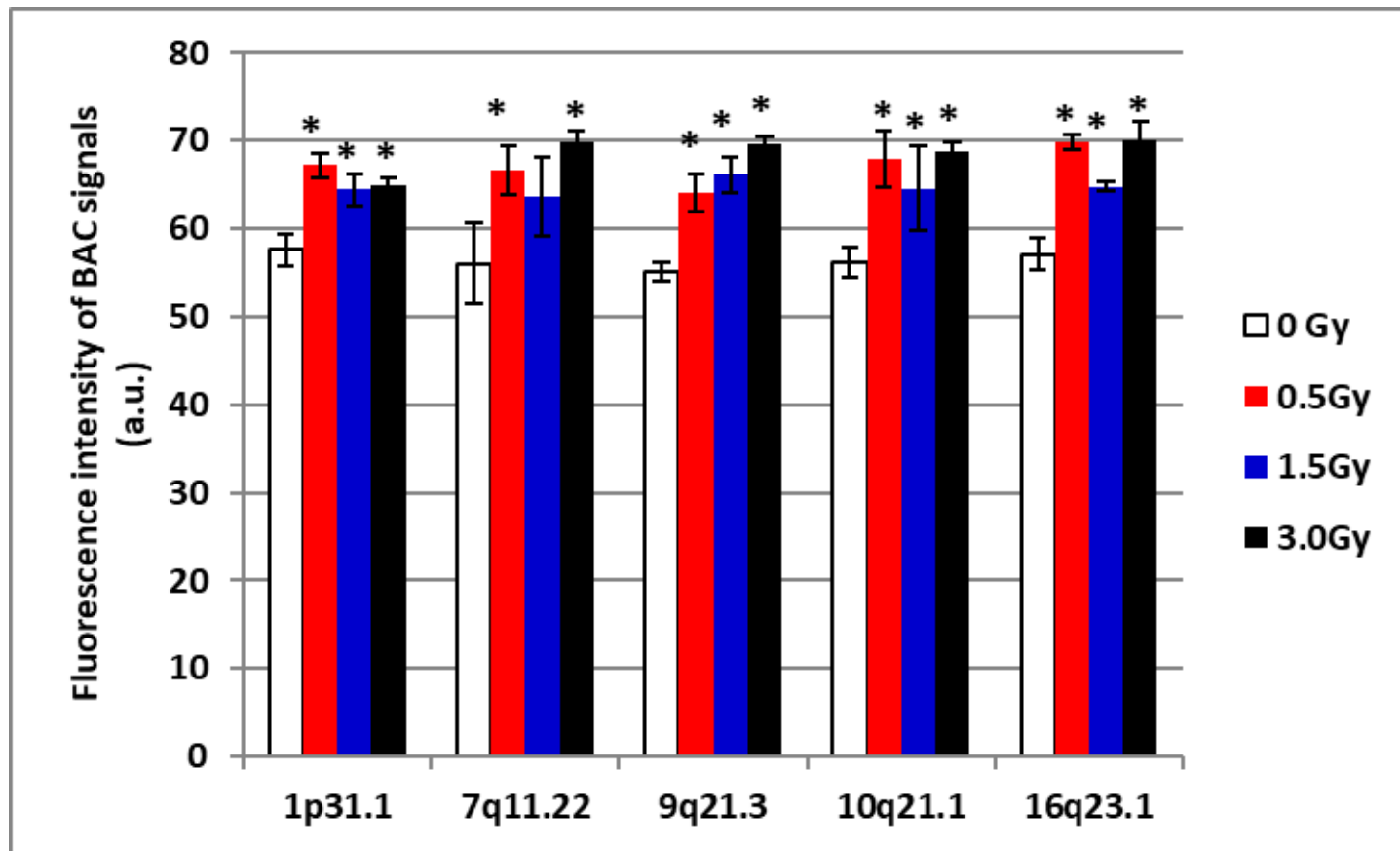
- **Mean fluorescence intensities of BAC signals at CNV loci** measured by ImageJ program.
- **Irradiation with 3 MeV, 2 Gy/min, 2 Hz**
- **Irradiation of cells with 0.5, 1.5 and 3.0 Gy significantly increased signal intensities (duplication or amplification) in all analyzed chromosomal regions compared to controls.**
- **At the dose of 3 Gy irradiation induced duplications at 9q21.3, 16q23.1 and 7q11.22, and deletion at 1p31.1.**
- ***-p<0.05 compared to control.**

Ionizing radiation (1.5-3 Gy) induces copy number variations (CNVs) of DNA sites.
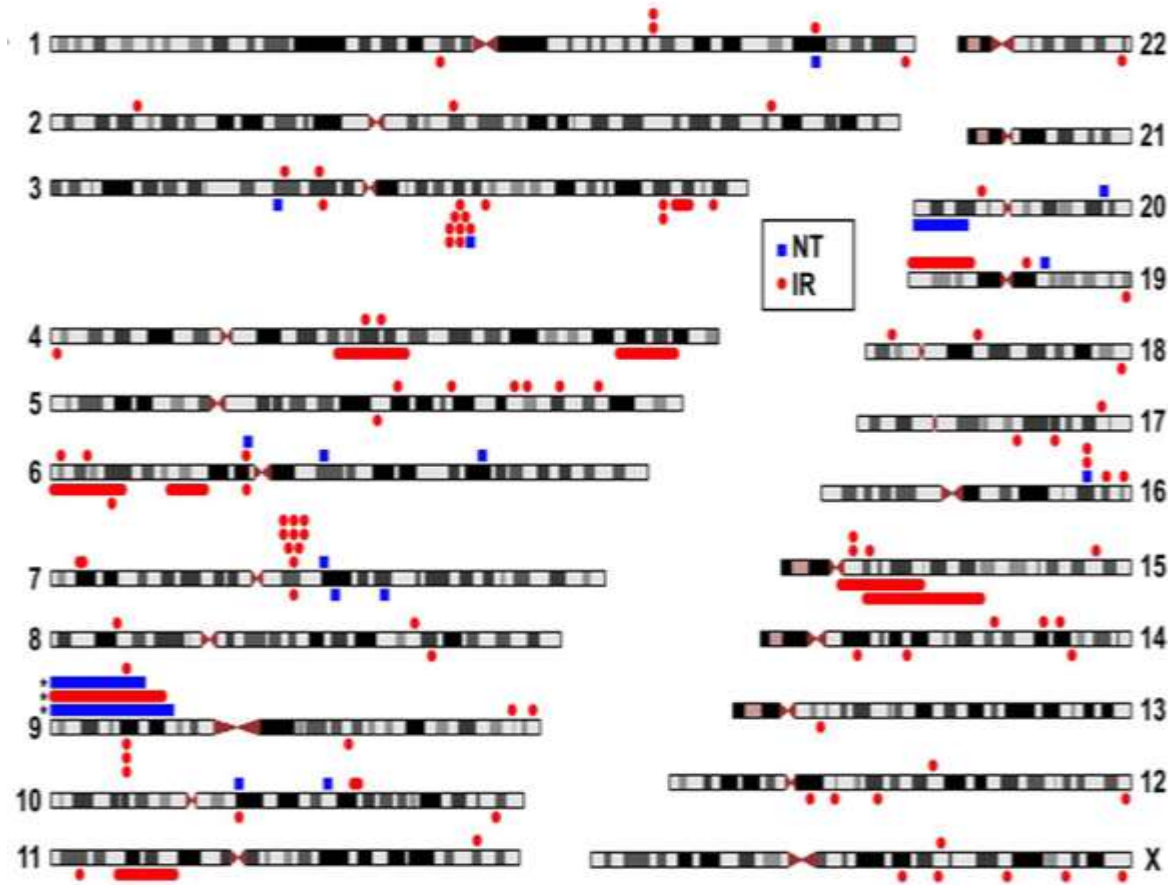
Arlt et al. Copy number variants are produced in response to low-dose ionizing radiation in cultured cells.
Environ Mol Mutagen. 2014; 55(2):103-13. Irradiation by Philips RT250 (Kimtron Medical)

Analysis of copy number variations induced by ultrashort electron beam radiation in human leukocytes in vitro

Tigran Harutyunyan [1], Galina Hovhannisyan [1], Anzhela Sargsyan [1], Bagrat Grigoryan [2], Ahmed H Al-Rikabi [3], Anja Weise [3], Thomas Liehr [3], Rouben Aroutiounian [1]

Affiliations + expand

PMID: 31131024   PMCID: PMC6524226   DOI: 10.1186/s13039-019-0433-5

➢**CNVs** occur most likely due to **duplications or amplification** and tend to **inversely** <u>**correlate with chromosome size and gene density.**</u>

➢CNVs **can last** in cell population as stable chromosomal changes **for several days after radiation exposure**; <u>**therefore this endpoint can be used for characterization of genetic effects of accelerated electrons!**</u>

Insertions of mtDNA sequences in chromosomes

Mitochondria are organelle found in large numbers in most cells, in which the biochemical processes of respiration and energy production occur.

Over 1000 NUMTs - nuclear DNA sequences of mitochondrial origin "**new mights**" **are present in human chromosomes.**

NUMTs can become amplified in the human genome as mega-NUMTs

Mitochondrial-nuclear genome fusion sequences are largely present in cancer cells.

Harutyunyan T, Al-Rikabi A, Sargsyan A, Hovhannisyan G, Aroutiounian R, Liehr T. Doxorubicin-Induced Translocation of mtDNA into the Nuclear Genome of Human Lymphocytes Detected Using a Molecular-Cytogenetic Approach. Int J Mol Sci. 2020

mt-DNA-FISH

Doxorubicin-induced translocation of mtDNA into the nuclear genome of human lymphocytes

MN assay
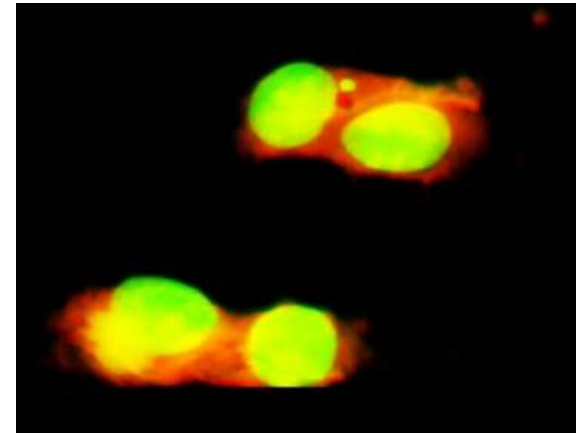
Doxorubicin

24 h treatment

mtDNA-FISH
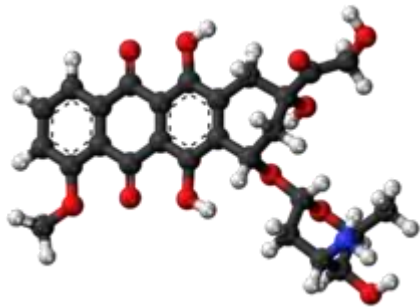
Doxorubicin

is antineoplastic drug for which radiation recall reactions have been most commonly reported. Radiation recall is an acute inflammatory reaction confined to previously irradiated areas that can be triggered when chemotherapy agents
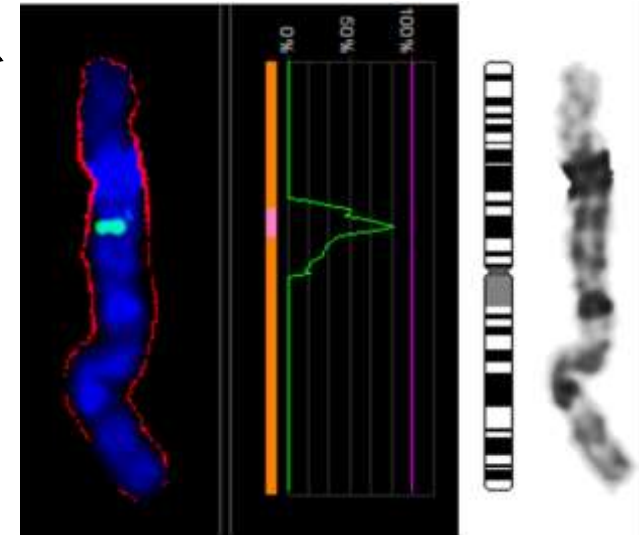
mtDNA-FISH in human chromosomes
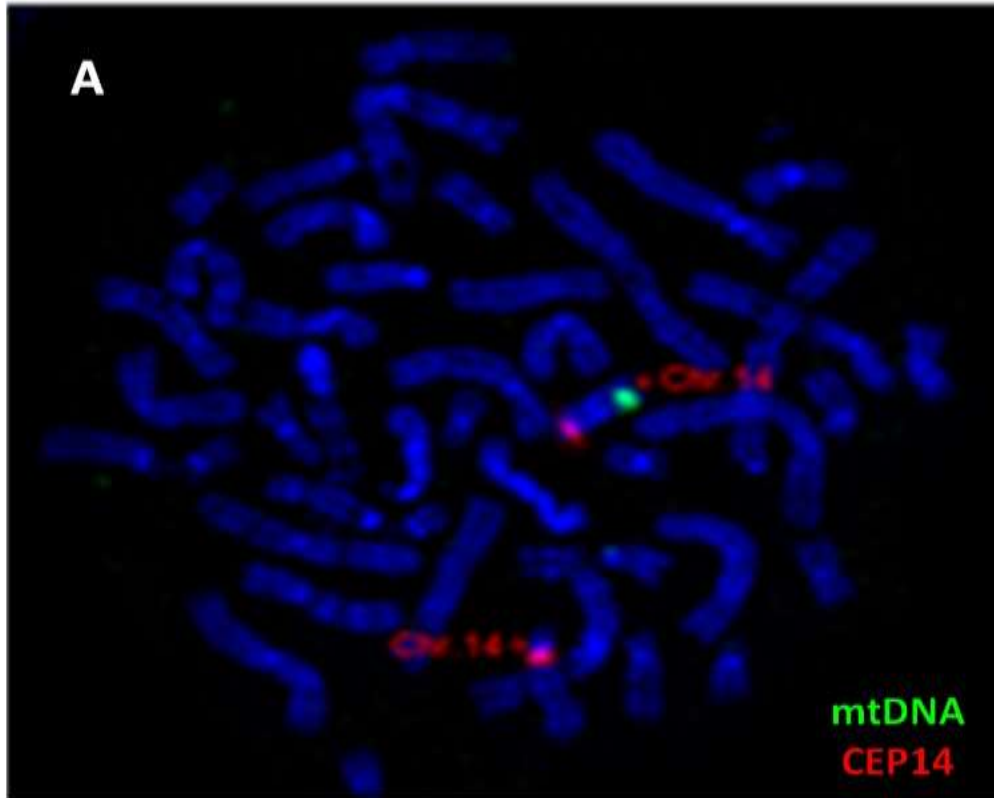
Positive control with mtDNA insertion in 14q31 of a healthy person
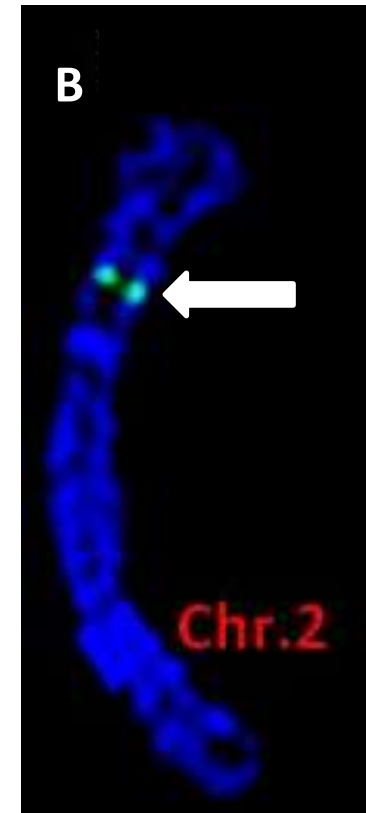
DOX-induced mtDNA insertion (green signals) on 2p21

Harutyunyan et al. *Int J Mol Sci*. 2020;21(20):7690

Further studies with novel biomarkers and modifiers of genomic instability
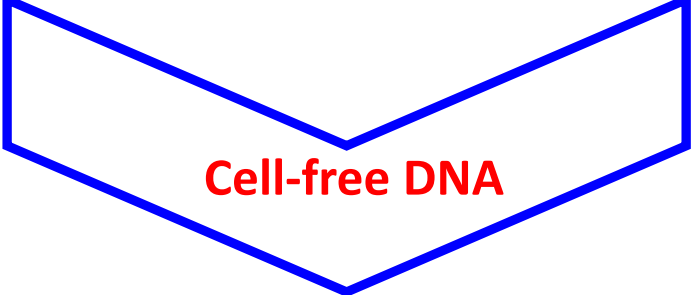
Cell-free DNA

Radiation exposure can induce long-lasting effects mediated by inflammatory reactions. One of recently identified inducers of inflammation **is mitochondria and mtDNA**. **The expulsion of mitochondria and mtDNA can elevate the inflammatory response in radiotherapy.**

The significance of **cell-free mtDNA in radiation is poorly studied**. In addition, studies of changes in gene expression, regulating **mtDNA release from mitochondria** can have significant impact for the **development of better radiotherapy approaches.**

Radiosensitizer is any substance that makes tumor cells easier to kill with radiation therapy
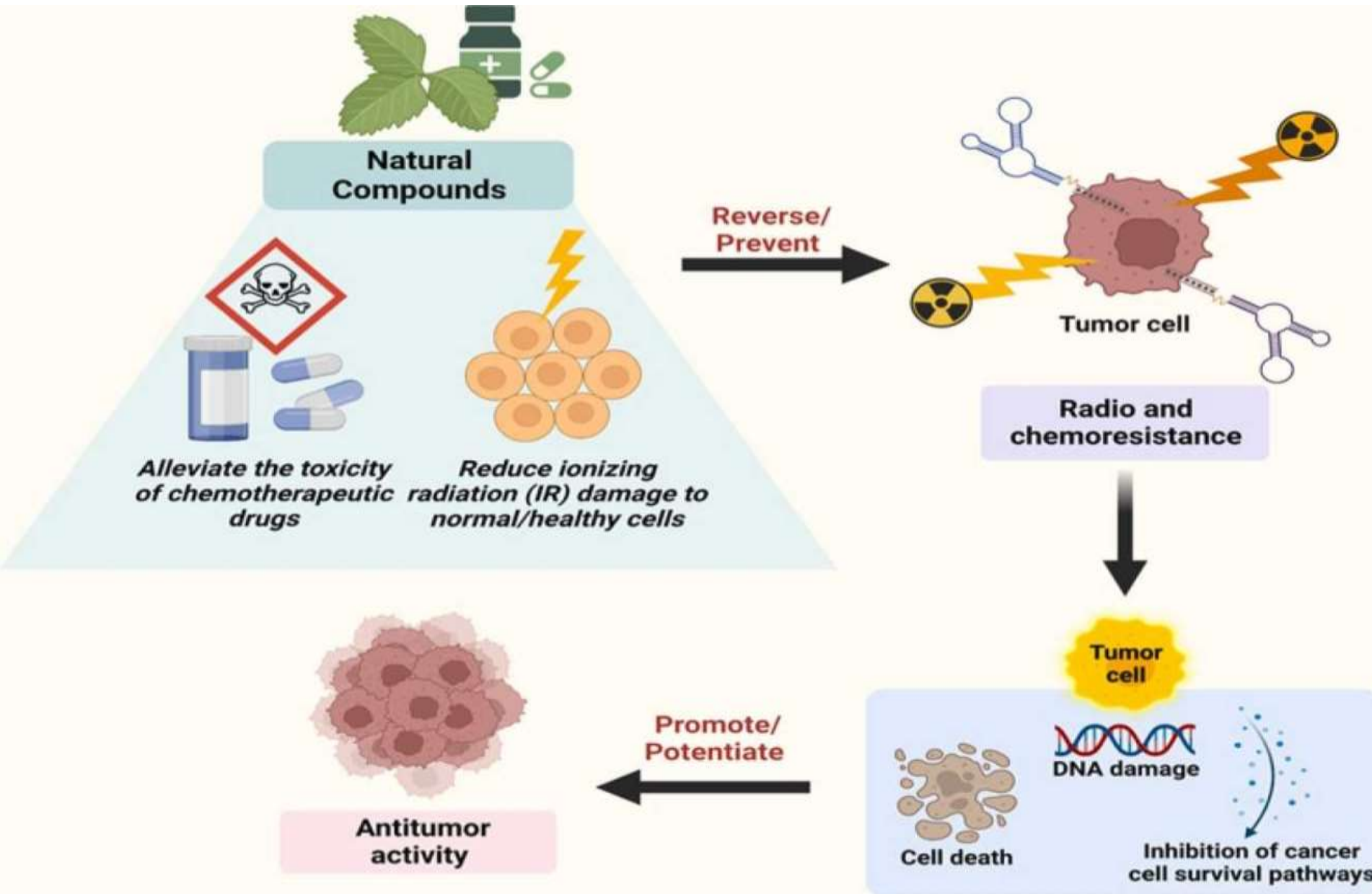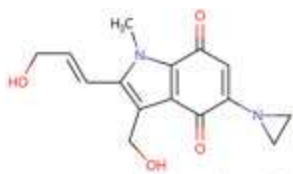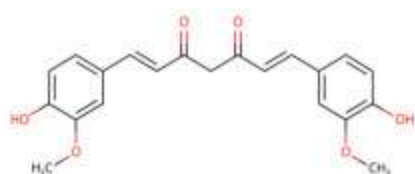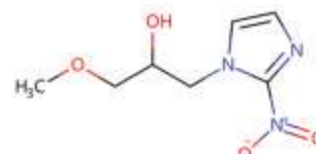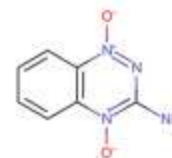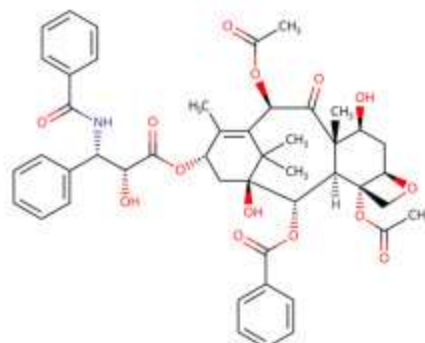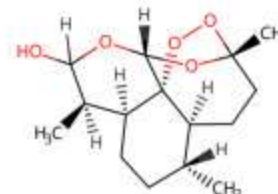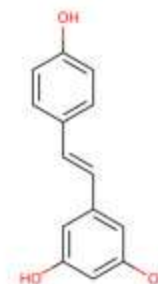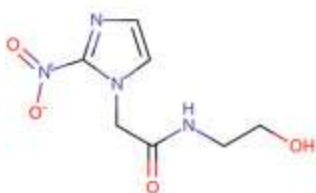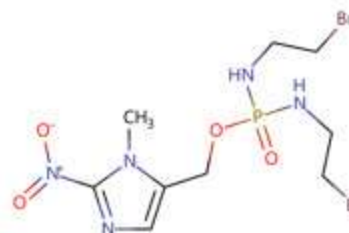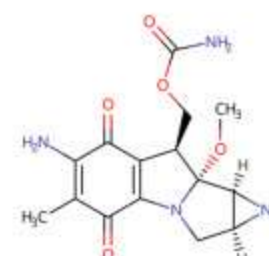
Molecular structures of some representative small-molecule radiosensitizers

Conclusions 2

Telomere lengths of human chromosomes,
copy number variation, mtDNA insertions in
nuclei can be considered as potential biomarkers of
electron beams inducing genomic instability.

Obtained results open good perspectives in radiotherapy

by further enhancing of their efficiency in tumour cells

compared with normal cells, by using radiosensitizers.

Acknowledgements

Prof. Galina Hovhannisyan

Dr. Tigran Harutyunyan

Dr. Nelly Babayan

Dr. Bagrat Grigoryan

Prof. Thomas Liehr

Prof. Andreyan Osipov

Dr. Natalia Vorobyeva

PhD student Alisa Manukyan

PhD student Anzhela Sargsyan

Acknowledgements

Best Wishes!

Biologic Modifiers of Radiation Response

Overexpression of the epidermal growth factor receptor 1 (EGFR-1) is associated with an adverse outcome in squamous head and neck cancer.

Cetuximab (C225) is a chimeric monoclonal antibody to EGFR.

Preclinical studies have demonstrated that cetuximab sensitizes cells to the cytotoxic effects of ionizing irradiation.

Preliminary studies demonstrated that this drug could be safely administered in conjunction with a course of RT for head and neck cancer

Phase III trial by Bonner et al concluded that for patients with LASCCHN, cetuximab plus radiotherapy significantly improves overall survival at 5 years Vs RT alone.

Chemotherapy

- Chemotherapeutic agents are often utilized in conjunction with radiation therapy for their radiosensitizing effect.

- Concurrent chemoradiation with **platinum agents**, particularly cisplatin, improves survival in numerous malignancies including head and neck cancer, cervical cancer and lung cancer.

- Multiple potential mechanisms for platinum-induced radio-sensitization have been proposed like :--

  - blocking DNA repair

  - inducing cell cycle arrest

Taxanes : widely employed along with RT in Rx of head and neck cancer , lung cancer, and oesophageal cancer.

These drugs facilitate radiation induced cell killing by synchronizing cell cycle and causing **cell cycle arrest in the radiosensitive G2/M phase**.

Fluoropyrimidines such as **5-fluorouracil** are commonly administered concurrently with radiation therapy for gastrointestinal malignancies because of their radiosensitizing effect.

Slowed repair of radiation induced double-strand breaks and alteration of cell cycle progression by fluoropyrimidines likely result in radio sensitization.

Как определить ФСД

Фактор снижения дозы при разных режимах (у нас это 2Гц и 20 Гц), вычисляли при сравнении доз, приводящих к определенному эффекту, как например произведение доз, которые приводят к 50% гибели клеток (EC50) после облучения.

Расчет поглощенной дозы

1 Гр — доза, при которой массе 1 кг передается энергия иониз. излучения в 1 Дж:

Таким образом Грей- это поглощенная доза :

$$D (kGy) = P (kW) \times T (s)/M (kg)$$

M-Масса определяется как произведение объема культуры на плотность

$$P (kW) = E (meV) \times I (mA)$$ где

P (kW) – средняя мощность

T (s) – длительность импульса

E (meV) – энергия

I (mA) – средний ток - кулон/секунду зависит от ГЦ, например, при 2 Гц перемножаем 180 кулон/секунду на 2

Comparison of DSB from different sourses

DSB yield of cells in mammals is about 25 times smaller than of single-strand breaks (SSB).

Presented are the dose dependent frequencies of formation of double-strand DNA breaks after irradiation with γ-rays and high-energy carbon ions. For both types of irradiation with increasing doses the DSB output increases linearly. Former studies had revealed, that in prokaryotic and mammalian cells exposed to ionizing radiation with different physical characteristics in overlethal and lethal doses is obtained linear dose dependence of DSB.

The biological effectiveness of carbon ions in formation DSB, is close to that induced by γ-irradiation.

Heavy charged particles by accelerated lithium ions exhibit greater biological efficacy than γ-radiation.

The value of the RBE of particles = Dγ / DLi, was 1.6 ± 0.1. Low-energy ions of lithium with LET of 20 keV /micrometer possess very high biological effectiveness compared with γ-rays.

Starting from 15-30 keV /m is the area of the LET values .

In the publication of Praveen (2014) on variation of Olive tail moment with dose for human peripheral blood cells after electron and gamma irradiation. coefficients, the values of the coefficients a and b were found to be 4.14 Gy^{-1} and 1.16 Gy^{-2}, respectively, for electron radiation; the corresponding values for gamma radiation were 4.57 ± 0.65 Gy^{-1}; 0.43 ± 0.19 Gy^{-2}
($R2 = 0.99$, $Chi^2 = 0.74$).
The gamma dose response on DNA damage induction is almost linear with a smaller quadratic component (a/b =10.6),
but for electron irradiation, the response is linear quadratic with a larger quadratic component.
This can be attributed to the high dose rate irradiation
(100 $Gy\ min^{-1}$) using electron, whereas the dose rate for gamma irradiation was 2 $Gy\ min^{-1}$.

Praveen electrons vs. Areal electrons

OTM	**Praveen *et al.*** Microtron accelerator **8 MeV**	**We** Areal accelerator **3,6 MeV**	RBE	Mean
	Electron dose, Gy			
10	1.5	3	2	
20	2.62	5,4	2.1	**2.1**
25	3.08	7	2.3	

Praveen et al. experiment - Radiation treatment has been carried out using electron beam from microtron accelerator at Mangalore University. It is a pulsed mode circular accelerator (*we – pulsed mode linear accelerator*) offering an electron beam with a maximum pulse current of 50 mA and pulse duration of 2.5 μs (*we-400 fs*), electron energy of 8 MeV (*we – 3.6 MeV*).

• **The SSB and DSB yields linearly depends on the electron beam energy !**

A comparison between levels of DNA damage in K-562 cells after 3 and 24 hours after irradiation, by Tail Moment (repetition rate **2 Hz and 20 Hz**)
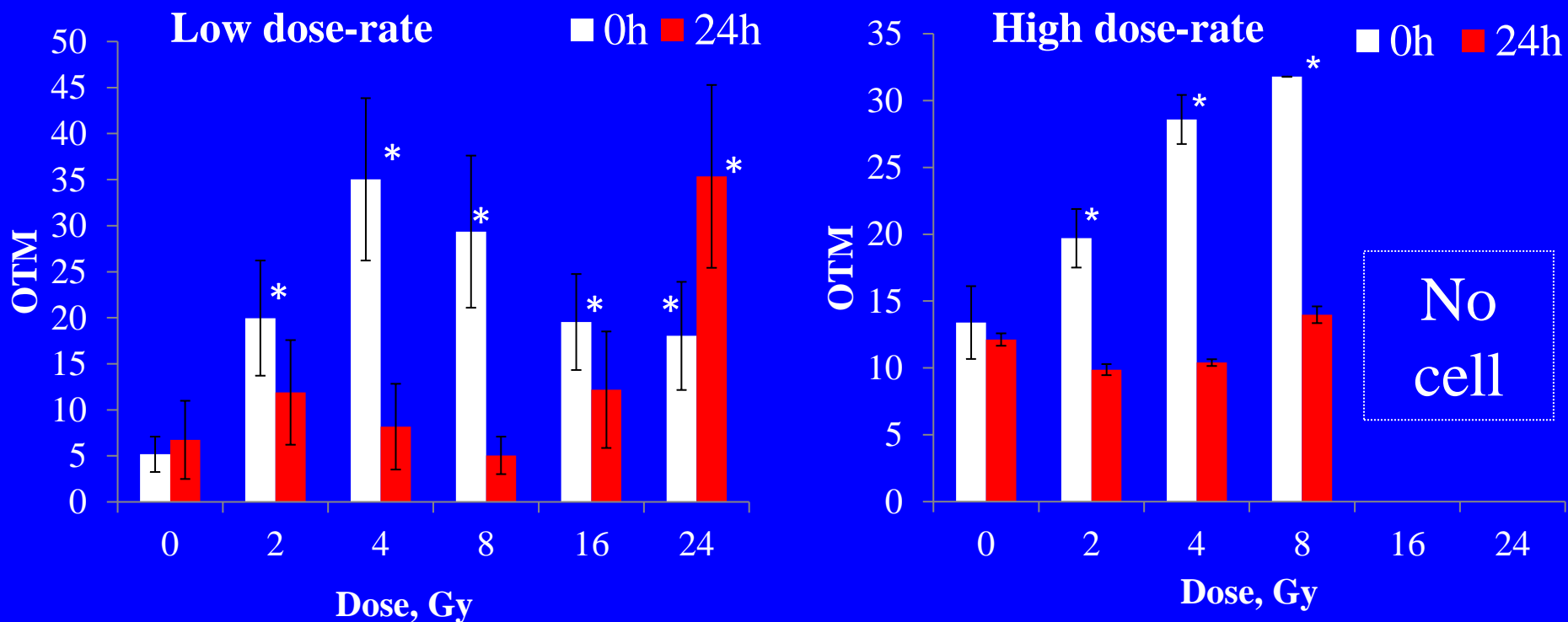
- Low dose-rate – 3,6 Gy/min (**repetition rate 2 Hz**)
- High dose-rate – 36 Gy/min (**repetition rate 20 Hz**)

The exposure of K562 human chronic myelogenic leukaemia cells to AREAL ultrafast electron irradiation at different doses revealed the dose-dependent increase of the primary DNA damage.

The comet assay was performed immediately after the irradiation to avoid DNA repair. Reparable and non-reparable DNA damages were assessed after 24h-incubation of irradiated cell culture.

The level of DNA damage was defined by <u>tail intensity</u> – the amount of DNA in the tail of the comet multiplied by median migration distance.

At the doses higher than 4 Gy the DNA damage decreases. The reason - the level of dead cells can be increased in relation to viable cells. After 24 hour of cell incubation, the damaged DNAs have repaired until 24 Gy.

It was shown that electrons, as a source of low LET radiation, led to isolated DNA lesions, including single-strand and double-strand breaks of DNA, which were generally repaired efficiently.
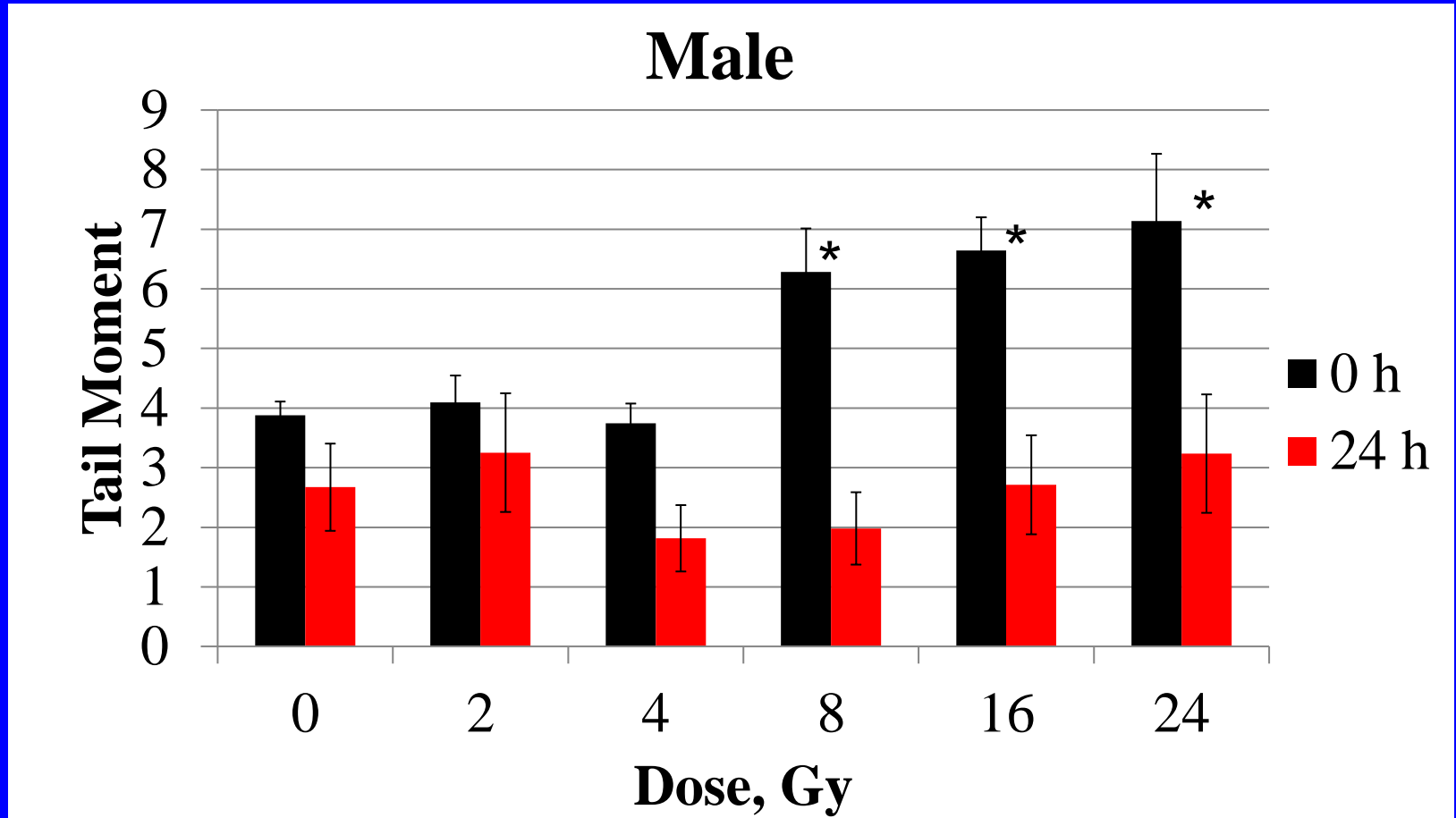
The level of DNA damage in male PBMCs at 0h and 24h post-irradiation with femto-second electron beam
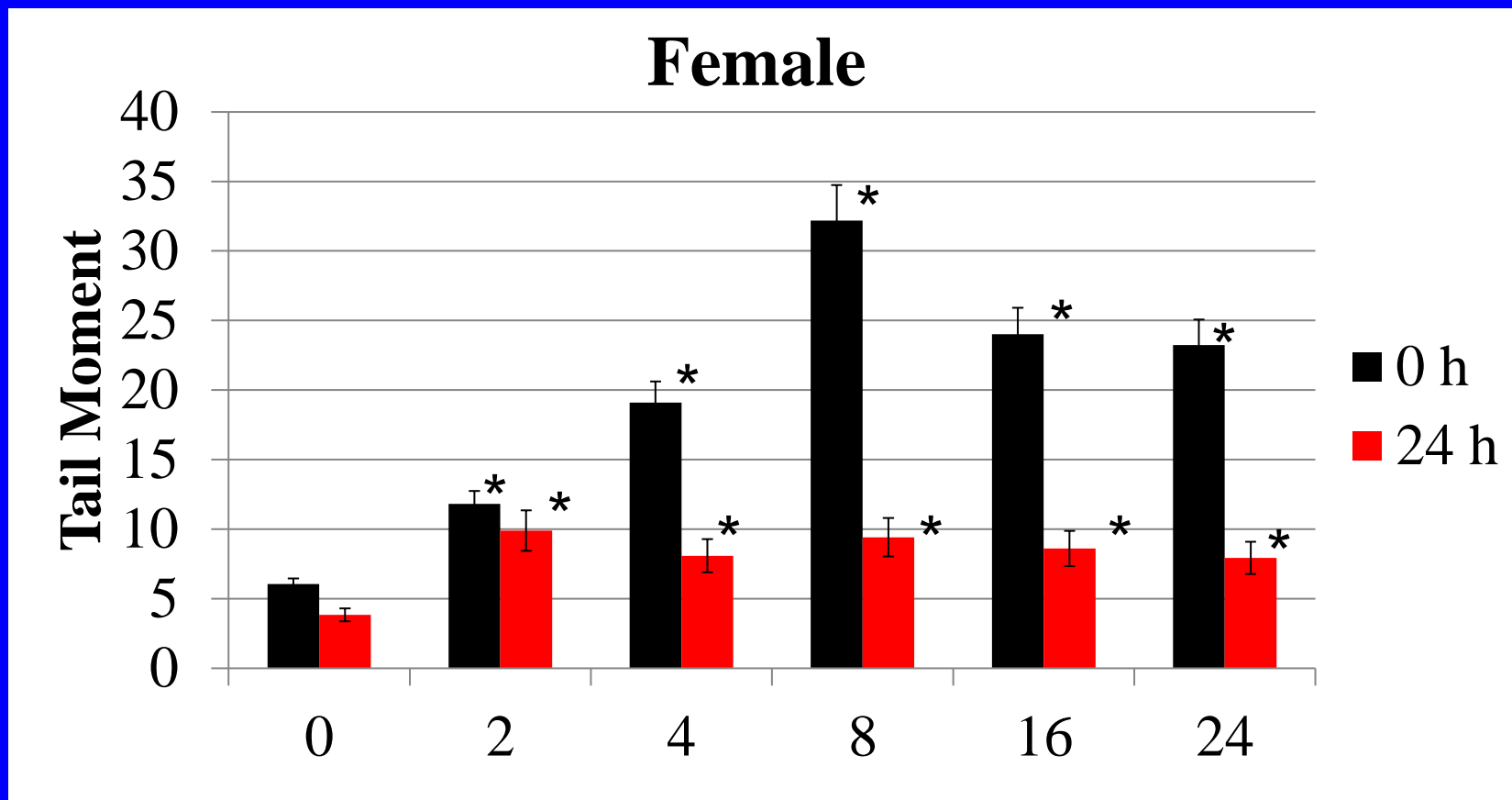
The level of DNA damage in female PBMCs at 0h and 24h post-irradiation with femto-second electron beam

The comparison between male and female PBMCs response to the irradiation was demonstrated, that female PBMCs are more sensitive, as the DNA-damage level in female PBMCs increased more than 5 times (8Gy) in comparison with negative control, which leads to the formation of unrepairable DSBs and SSBs.

In male's cells even at the highest dose of irradiation (24Gy) the level of DNA-damage increased less than 2 times in comparison with negative control, and those damages was totally repairable.
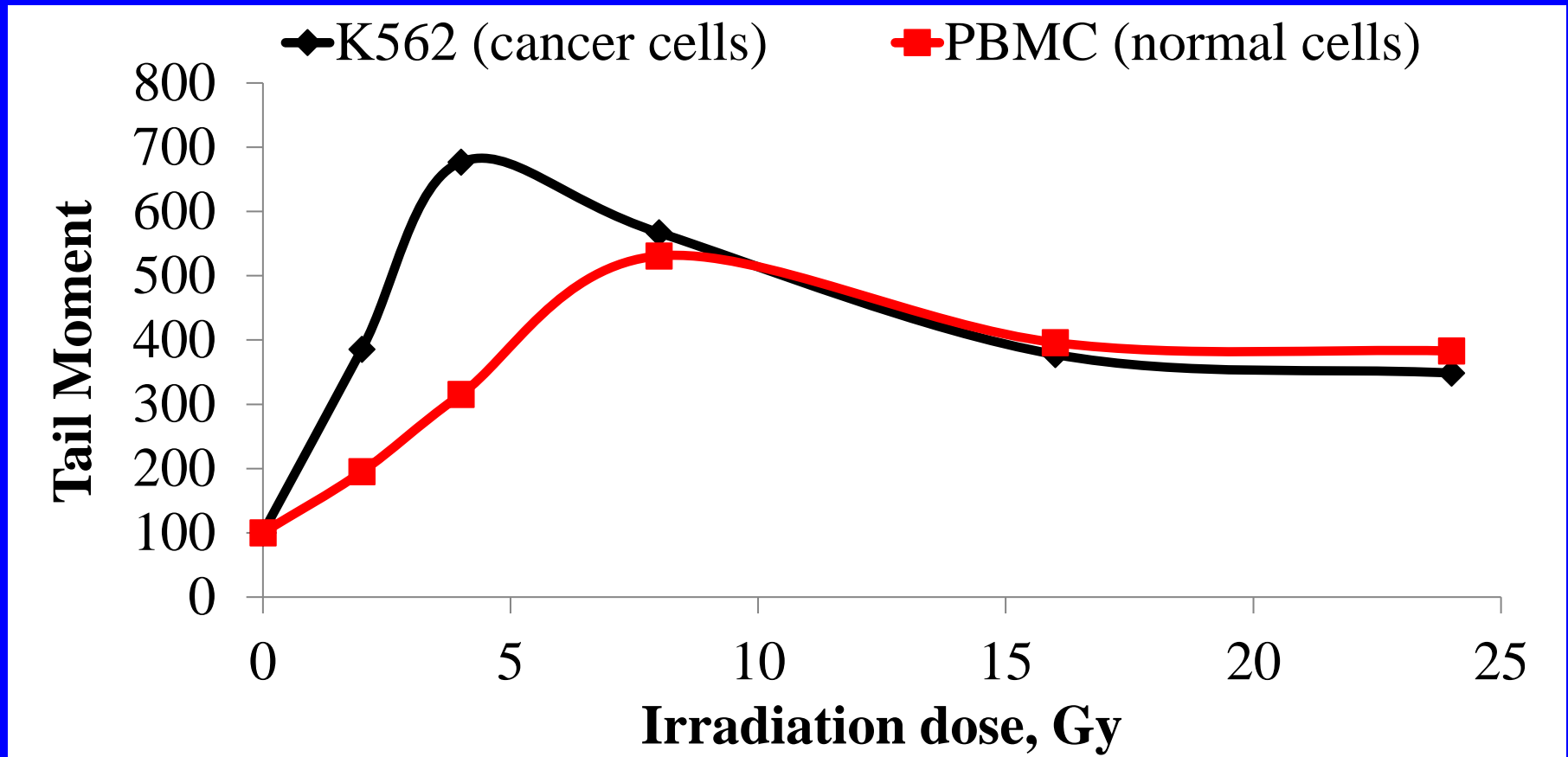
The level of DNA-damage in female PBMCs (blood normal cells) and K562 cell line (blood cancer cells, female) after 3 hour of irradiation with femtosecond electron beams

For comparison of cancer and normal cells the female data were used, as the cancer cell line K562 was also obtained from female.

In the case of normal and cancer cells, a hormesis effect was evidenced, followed by a linear dependence of the dose-effect. Neoplastic cells show higher effects at the doses of 2-4Gy of irradiation, but starting from 8Gy the similar behavior between normal and cancer cells response was evident.

By Borcia et al.,2014 "The slopes of dose-effect dependences for Olive Tail moment ,calculated by linear interpolation, are 0.31 Gy^{-1} for normal cells and 2.59 Gy^{-1} for neoplastic HeLa cells. These values suggest that <u>normal cells are less damaged by radiation than neoplastic ones, which is a good aspect in case of cancer treatment using electron beams."</u>

Proton Therapy

<u>Proton therapy is a type of radiation that utilizes a particle, the proton, to deliver radiation while minimizing dose to nearby organs</u>. The prevalence of proton therapy has dramatically increased in the past decade as technology has improved. However, this treatment is still not widely available because the machines that produce and deliver protons, are extremely large (about 3 stories in height) and are very expensive. Smaller machines are in development, which make this treatment available in more locations.

<u>The advantage of protons is that the depth at which they release their energy can be precisely controlled.</u> As the proton enters the body, it releases small amounts of energy, and slows down. At the end of its path, it releases a large amount of energy, and very little energy is released past that point. Using computer software, the protons can be directed to release their energy precisely within the tumor, without any of the energy exiting out of the back of the tumor. Hence, if the back edge of the tumor is located against the spinal cord, it may be possible to spare any radiation dose to the spinal cord using protons.

<u>The disadvantages to protons are mostly related to their limited availability, which may delay or preclude treatment for patients.</u>

LINAC

The advantage of linear accelerator radiation therapy is that it can target the tumor without affecting the surrounding tissue. This process makes the linear accelerator radiation therapy better on the patient and more effective in treating the specific cancer without the side effects of damaging the healthy tissue.

Medical grade LINACS accelerate electrons using a tuned-cavity waveguide, in which the RF power creates a standing wave. Some linacs have short, vertically mounted waveguides, while higher energy machines tend to have a horizontal, longer waveguide and a bending magnet to turn the beam vertically towards the patient.

Medical linacs use monoenergetic electron beams between 4 and 25 MeV, giving an X-ray output with a spectrum of energies up to and including the electron energy when the electrons are directed at a high-density target. The electrons or X-rays can be used to treat both benignand malignant disease.

В линейном ускорителе электроны, т.е. отрицательно заряженные частицы, ускоряются с помощью высокочастотного излучения и могут непосредственно использоваться для облучения опухолей. Поскольку электроны не способны глубоко проникать в ткани, их применяют, например, для лечения кожных опухолевых заболеваний.

Для облучения злокачественных новообразований, расположенных в более глубоких слоях тканей, необходимо использовать фотонное излучение. Когда ускоренные электроны сталкиваются с препятствием (мишенью), изготовленным из тяжелого металла, чаще всего вольфрама, это сопровождается выработкой высокоэнергетического рентгеновского излучения. Чем мощнее фотонное излучение, тем больше глубина его проникновения в ткани.

Electron Radiation

Electrons are a different form of radiation than photons and have different physical properties, but work biologically the same as photons. Linear accelerators, in addition to producing photons, can also produce electrons; consequently electrons are available at most treatment centers. Electrons tend to release their energy close to the skin's surface and are commonly used to treat superficial tumors, such as skin cancers and superficial lymph nodes, which may be involved with tumor, such as in breast cancer, hence the radiation does not penetrate much past the skin to deeper normal tissues. This treatment has generally replaced orthovoltage because it can be combined in the same machine as a linear accelerator.

Areal

The RF gun is driven by doped laser system capable to provide about 200 μJ energy at 258 nm wavelength with a 0.4-9 psec pulse duration.

The nominal electron beam parameters range is: energy 2-5 MeV, bunch charge 10-250 pC, repetition rate 1-50 Hz.

The diagnostic tools include the magnetic spectrometer, Faraday cups, YAG screens and pepper port for the beam energy, energy spread, charge, beam profile, emittance measurements and control.

Parameters of the laser-accelerated electron beam

Dosimetric parameters	Doses	Dose rate	Beam charge	Electron energy	Laser pulses		Beam spot	Online Dose information
					duration	repetition rate		
Areal	2-24 Gy	3.6 MeV-1x10 $^{-4}$ Gy	10-250 pC	2-5 MeV	0.4-9 psec	1-20 Hz	3-6 mm	Faraday cup

- **ELBE**

- (Electron Linac for beams with high Brilliance and low Emittance) was used to mimic the **quasi-continuous electron beam of a clinical linear accelerator (LINAC)** for comparison with electron pulses at the

- ultra-high pulse dose rate of 10^{10} Gy min $^{-1}$
- **-either at the low frequency of a laser accelerator**
- **-or at 13 MHz avoiding effects of prolonged dose delivery.**
- The impact of pulse structure was analyzed by clonogenic survival assay and by the number of residual DNA double-strand breaks remaining 24 h after irradiation of two human squamous cell carcinoma.
- **Response of both cell lines was independent from electron pulse structure for the two endpoints.**

REGAE - FEL
Relativistic Electron Gun for Atomic Exploration

- The novel **source of relativistic electron beams** REGAE is a joint project of the CFEL partners Max Planck Society, University of Hamburg and DESY.
- The nearly ten-metres-long facility **generates ultra short electron pulses** of extremely high quality for time-resolved diffraction experiments
- The current design is capable of 7 femto-second electron pulses with up to 10^7 electrons per pulse
- Accelerates the electrons to energies of up to 5 MeV

- **REGAE** the Relativistic Electron Gun for Atomic Exploration is a small electron accelerator build and operated within the framework of the Center for Free-Electron Laser Science CFEL, i.e. in a collaboration of the Max Planck Society, the University of Hamburg and DESY.
REGAE provides high quality electron bunches for time resolved diffraction experiments and serves as test bed for accelerator R&D.

- REGAE employs a photo cathode RF gun operated at 3 GHz (S-Band) for the production of electrons. The 1½ cell gun cavity, a scaled version of the cavity in operation at the FLASH FEL, accelerates the electrons to energies of up to 5 MeV.

- Extraordinary emittance requirements in the nm range (normalized) and pulse lengths down to a level of ~10 fs require operation at low bunch charges on the sub-pC scale.

- **The current design is capable of 7 femtosecond (rms) electron pulses with up to 10^7 electrons per pulse with spatial coherence of over 30 nm.**
Femtosecond Electron Diffraction (FED) has the potential to directly observe the most venerable concepts in chemistry and biology most notably enabling a direct atomic level view of transition states. The relevant motions for this barrier-crossing event occur on the sub-hundred femtosecond time-scale which is addressed by pump-probe type experiments. The advantage of relativistic electron diffraction as compared to the more common diffraction with electron energies in the 100 keV range are reduced space charge effects and the higher penetration depth of the electrons.

- **<u>The Versatile Electron Linear Accelerator (VELA)</u>**

- A world leading, ultra-high performance electron beam injector system

- Ultra short electron pulses, down to below 100 femtoseconds

- Ultra high beam position and timing stability

- The unique ability to precisely tailor the electron beam, experimental configuration and shielding to match your requirements

- Opening Q2 2013

- Accelerator Science and Technology Centre
Sci-Tech Daresbury

Versatile Electron Linear Accelerator (VELA) parameters

- Beam Energy
- 4 – 5.5 MeV
- Bunch Charge
- 10 – 250 pC
- Bunch length (s t,rms)
- 80 – 3 ps
- Normalised emittance
- 0.1 – 2.0 mm
- Beam size (s x,y,rms)
- 0.1 – 3.5 mm
- Energy spread (s e,rms)
- 0.1 – 5 %
- Bunch repetition rate
- 1 – 10 Hz
-
-
- .

Data distribution of comet assay is usually asymmetric and therefore the use of the t-test is not adequate, and the use of Mann-Whitney test is preferable, but provides insufficient information. We can assume the distribution of comet assay data is a mixture of two distributions - normal, and exponential. However, that mixture is difficult to characterize.

Di Giorgio et.al. (2004). Evaluation through comet assay of DNA damage induced in human lymphocytes by alpha particles. Comparison with protons and Co-60 gamma rays.

Thin samples of human peripheral blood were irradiated with different doses (0 – 2.5 Gy) of 20.2 MeV helium-4 particles in the track segment mode, at nearly constant LET. Data obtained were compared with the effect induced by 4 MeV protons and Co-60 gamma rays.

$$f(T) = \frac{\beta}{\eta} \left(\frac{T}{\eta} \right)^{\beta-1} e^{-\left(\frac{T}{\eta} \right)^{\beta}}$$

The two-parameter Weibull model implies, that the probability density function has the following dependence:where, α is the scale parameter or characteristic value of the variable x, here the OTM, and β is the shape parameter.

The integral of the probability density function f(x) is the probability distribution P(x). The probability distribution is normalized so that the total area under the curve equals one.
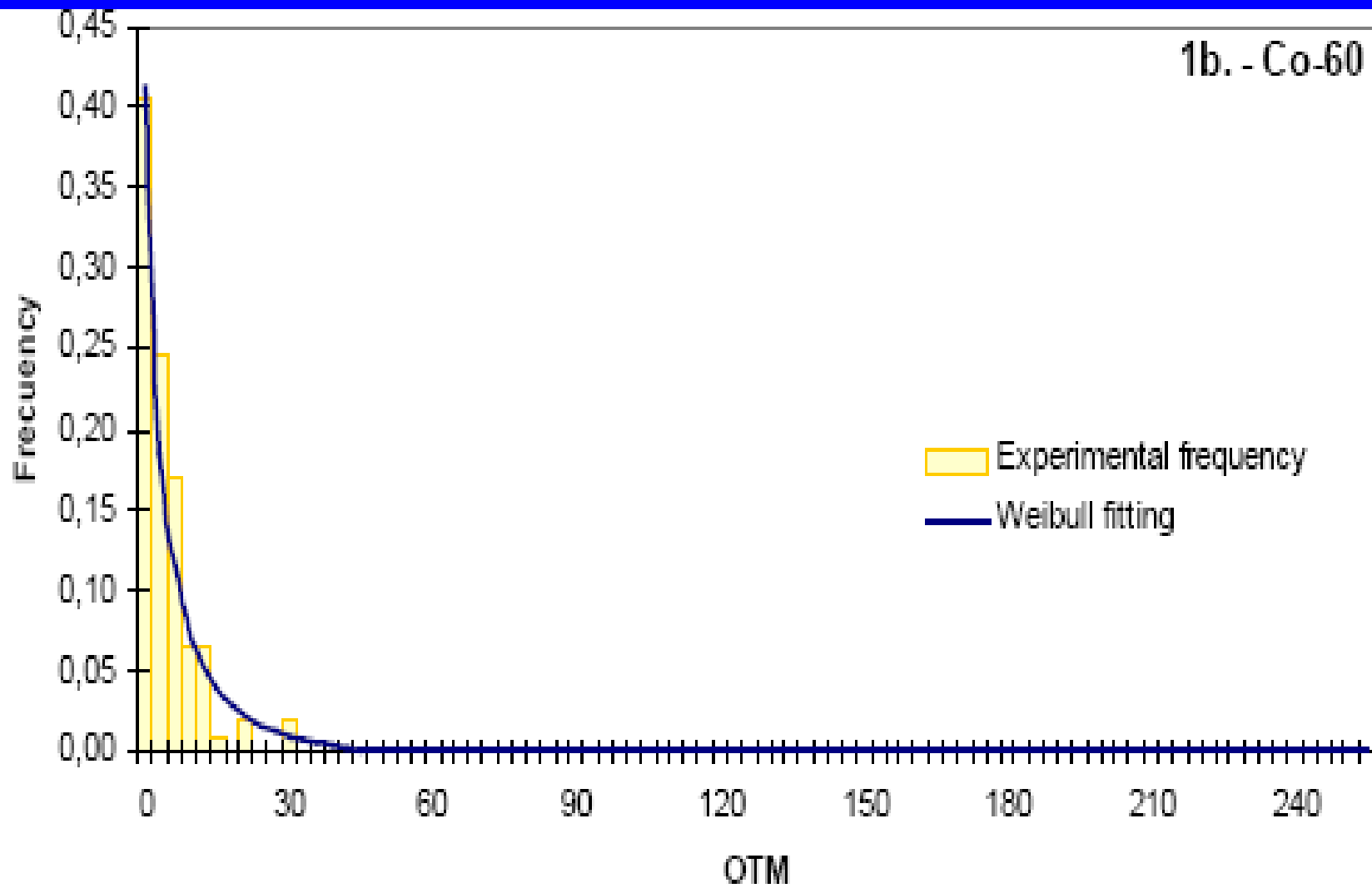
1d.- Alpha particles
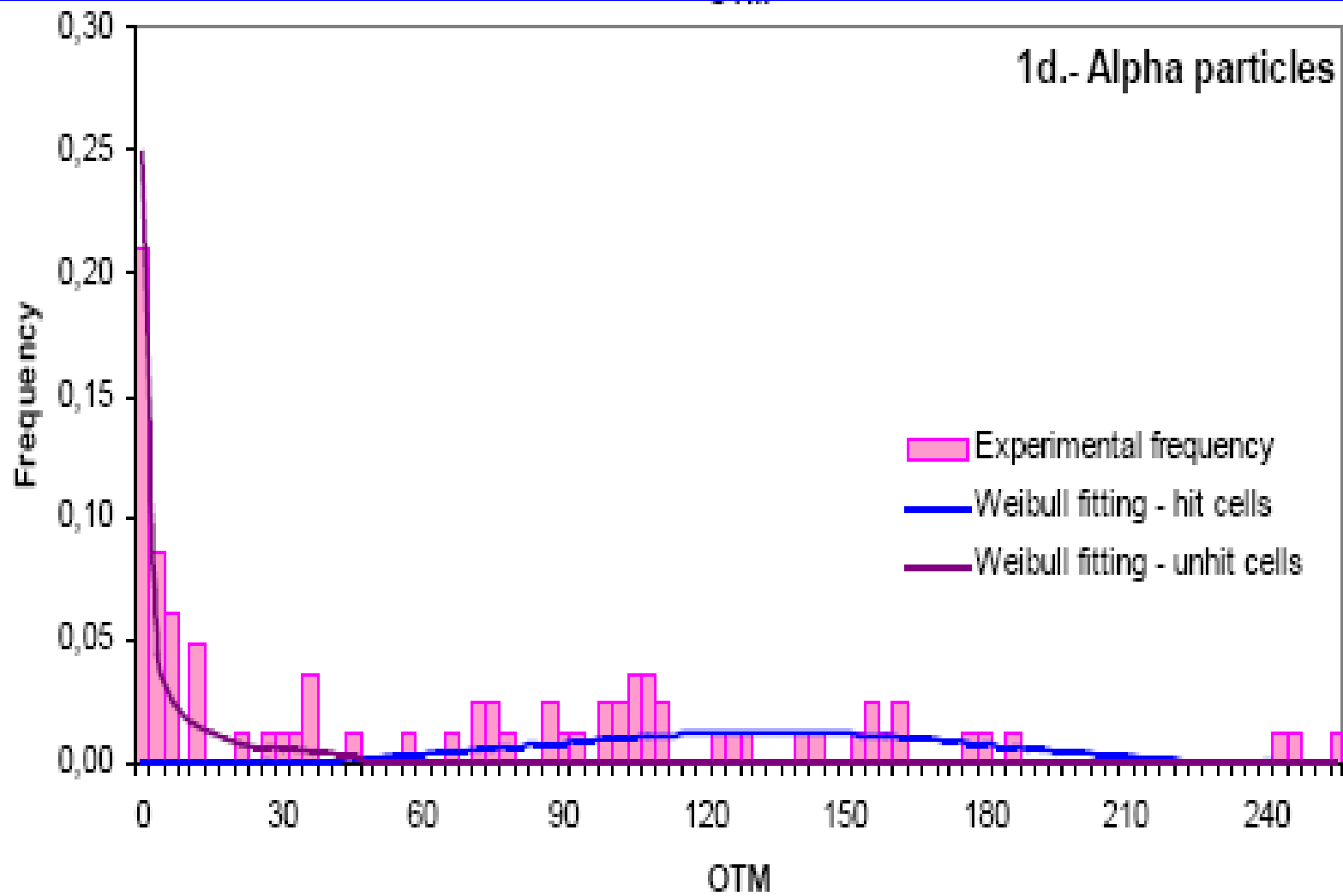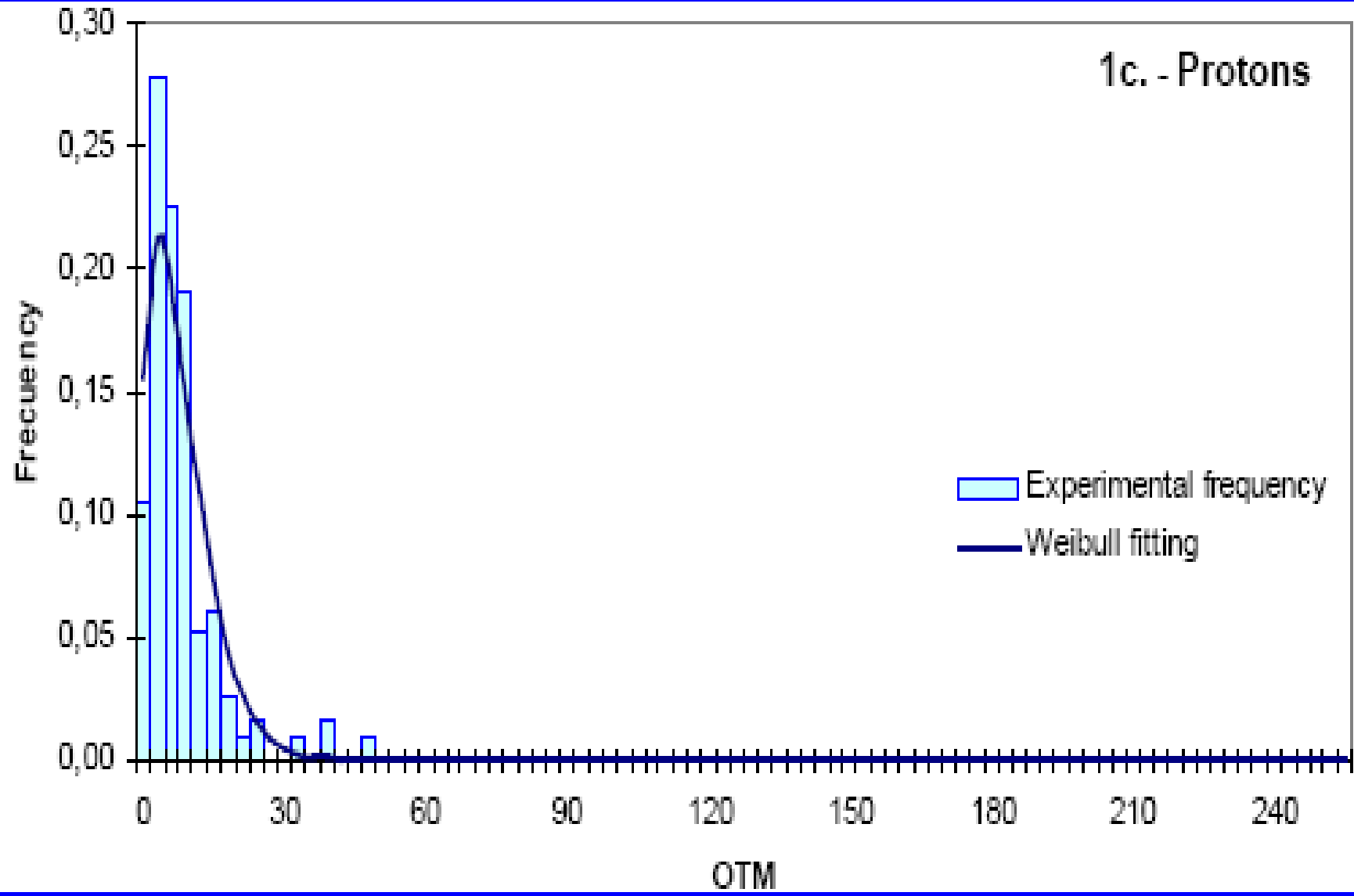
With helium-4 irradiations, lymphocyte nuclei show an Olive tail moment distribution flattened to higher tail moments.

For irradiations with protons and Co-60 -gamma rays, at increasing doses the tail moments are shifted towards high values with the same distribution, characterized by its asymmetry.
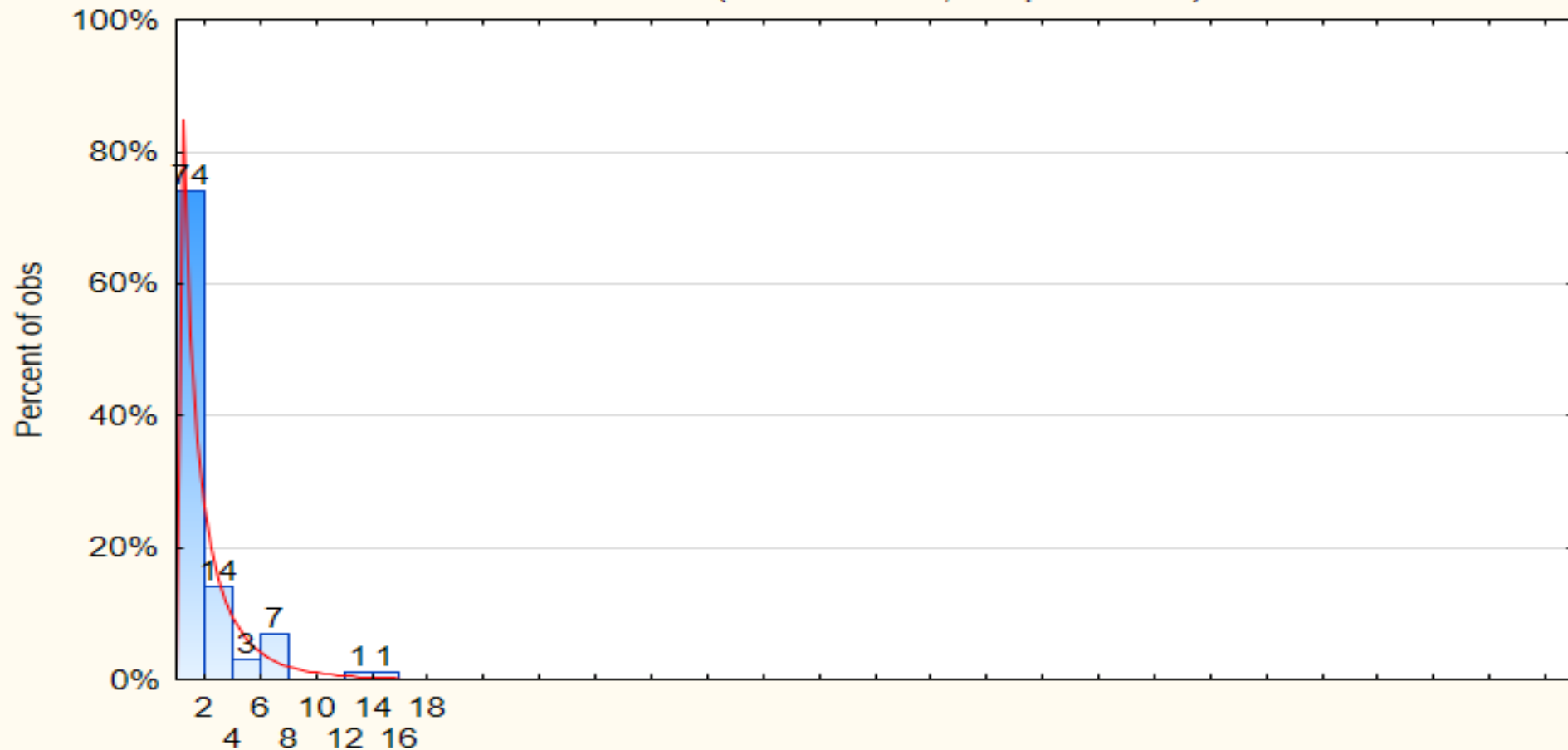These marked variations in DNA damage suggest that each lymphocyte nucleus might be crossed by different number of particles, increasing doses induce more breaks in every cell, resulting in a shift of comet distribution with the same profile.

Distribution of comets,8Gy,2 Hz
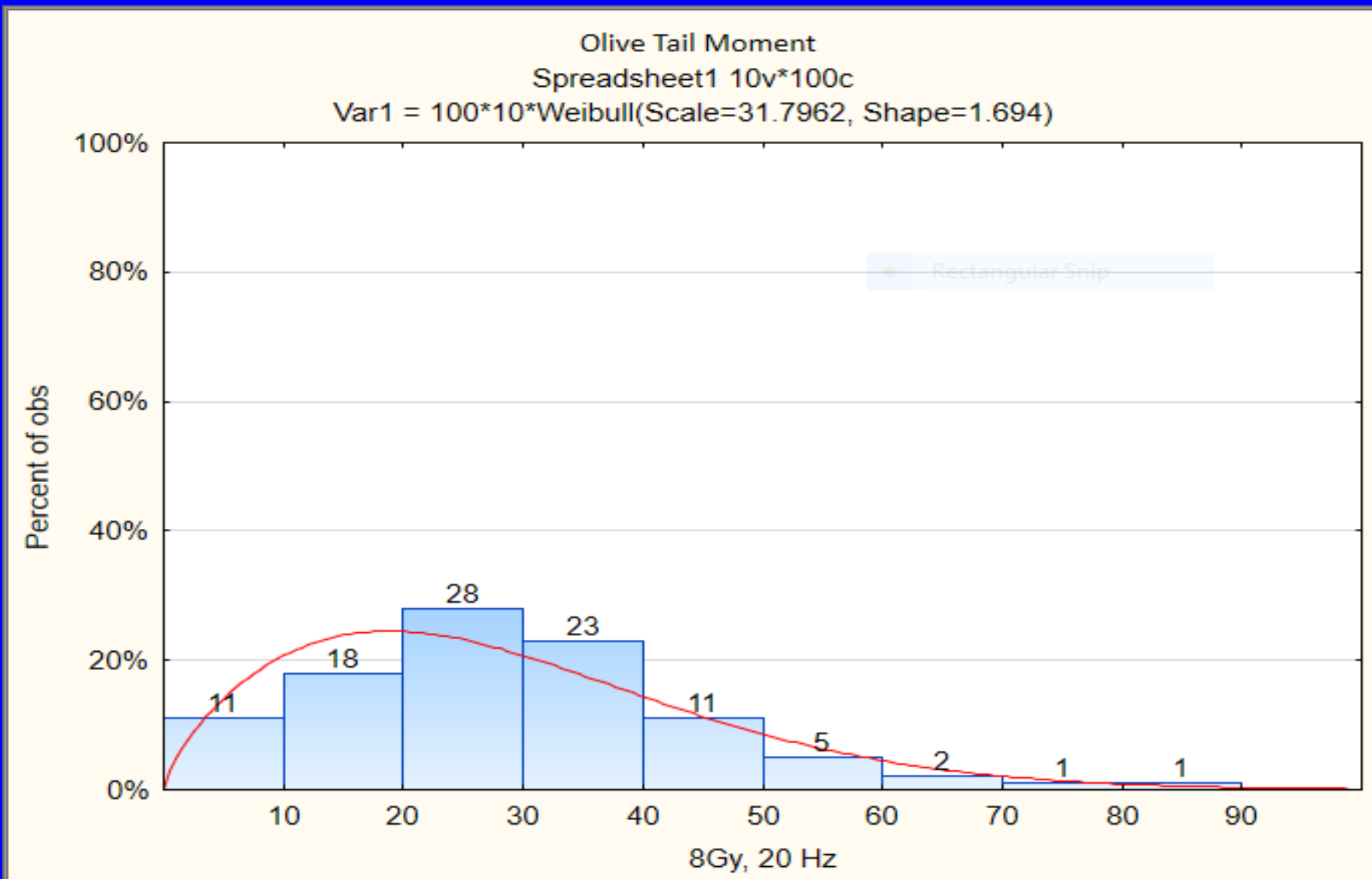

Olive Tail Moment
Spreadsheet1 10v*100c
Var1 = 100*2*Weibull(Scale=1.4676, Shape=0.7367)

8 Gy, 2 Hz

Distribution of comets,8Gy,20 Hz

Olive Tail Moment
Spreadsheet1 10v*100c
Var1 = 100*10*Weibull(Scale=31.7962, Shape=1.694)

RADIATION DAMAGE TO DNA

H2-Bond Breakage

Double-Strand Break

Pyrimidine Dimer

Base Loss

Base Change

DNA Cross-Linkage

Cross-Linkage

Single-Strand Break

Protein Cross-Linkage

4341-3
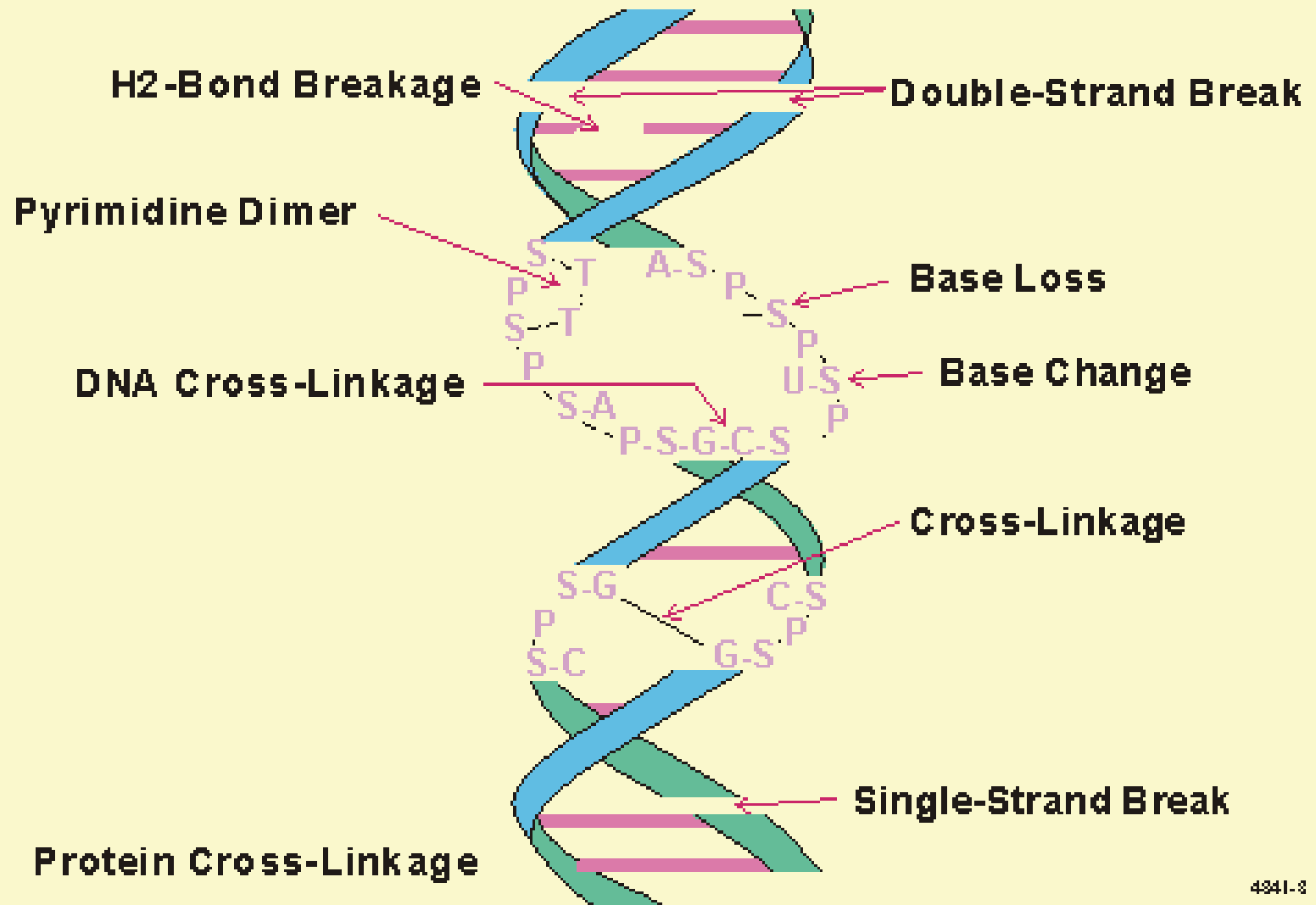
Comet analysis

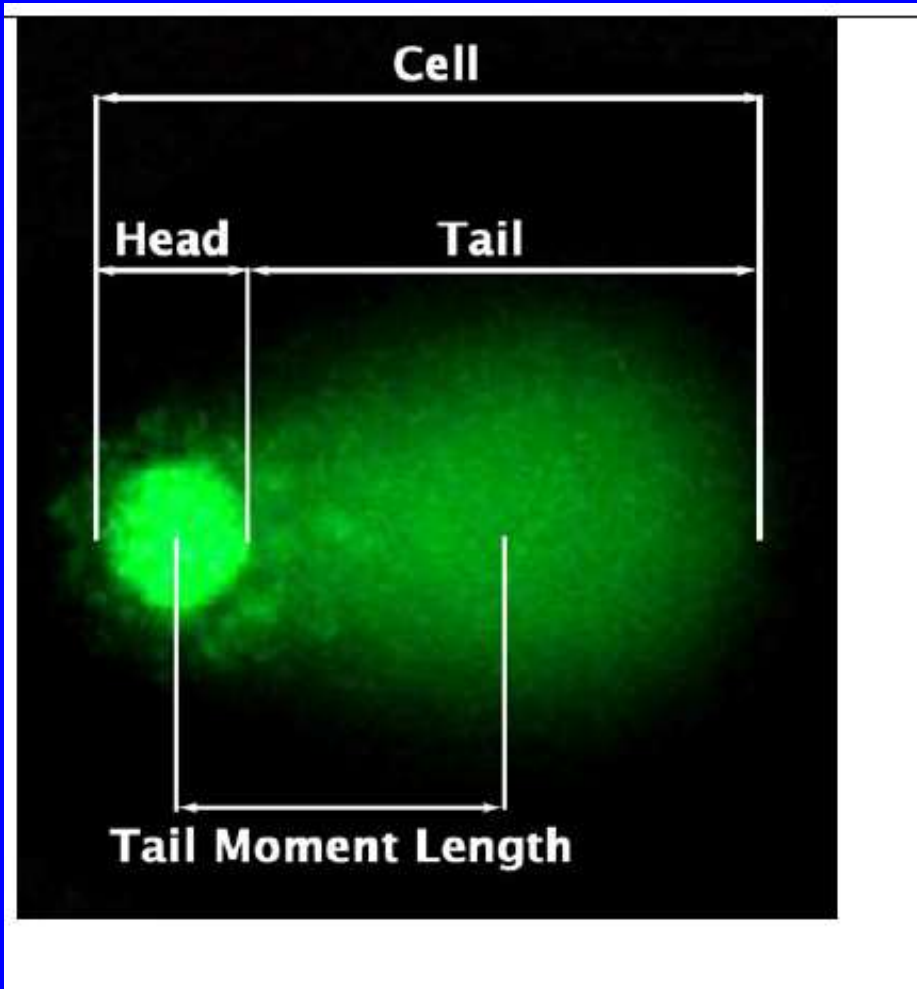Tail DNA% = 100 x Tail <u>DNA Intensity/Cell DNA Intensity</u>

Tail Moment can be measured using one of the following methods:
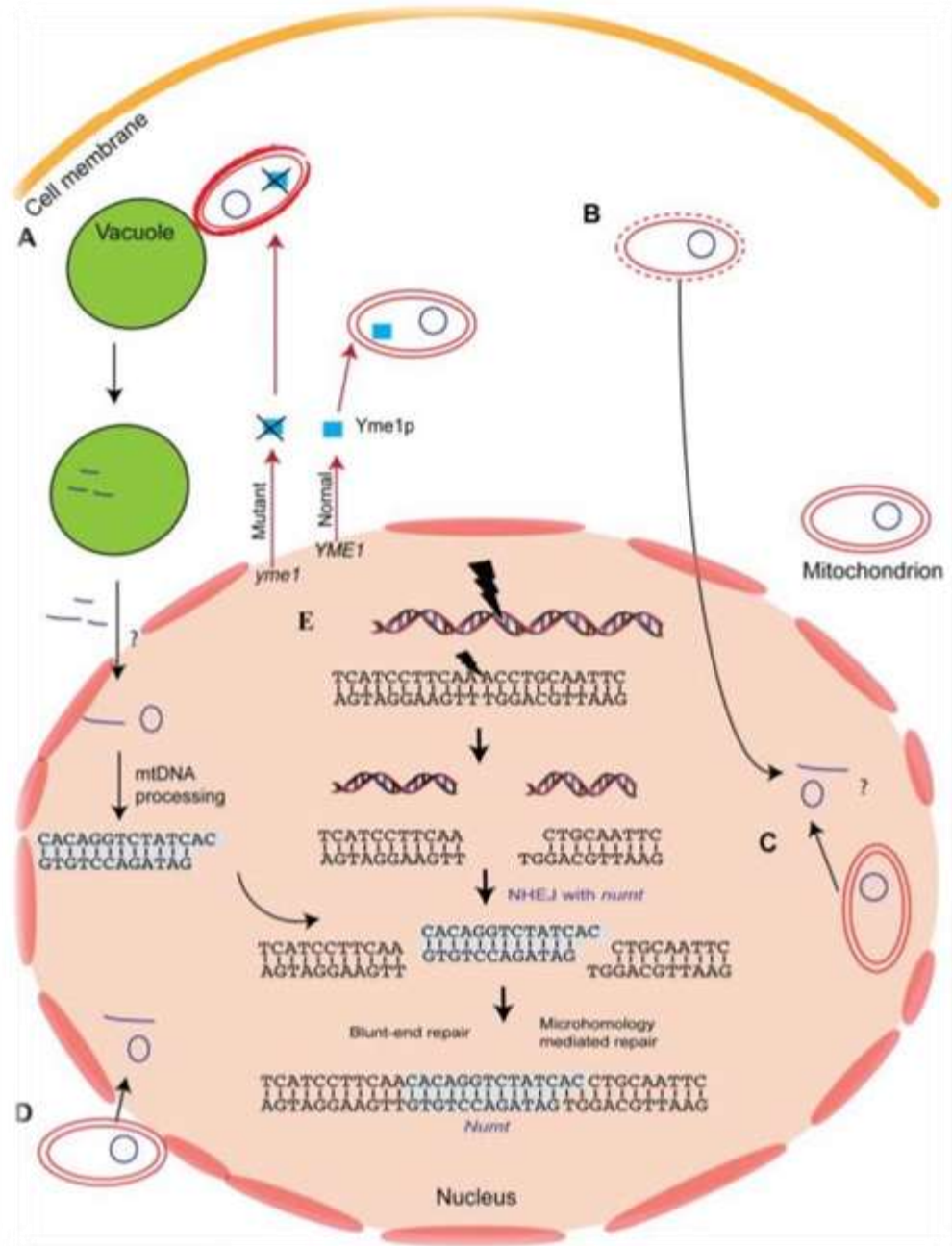
Tail Moment = Tail DNA% x Length of Tail (see diagram on left)

Olive Tail Moment = Tail DNA% x Tail Moment Length*

Tail Moment Length is measured from the center of the head to the center of the tail (see diagram)

Insertion of mtDNA in chromosomes mediated by DNA double strand breaks

Mitochondrial DNA has been suggested to get into the nucleus via a few different pathways. (A) The most supported pathway so far involve the degradation of abnormal mitochondria. Several yme (yeast mitochondrial escape) strains show high level of DNA escape to the nucleus. yme1 mutant cause the inactivation of YMe1p protein, a mitochondrial-localized ATP-dependent metalloprotease leading to high escape rate of mtDNA to the nucleus. Mitochondria of yme1 strain are taken up for degradation by the vacuole more frequently than the wild-type strain.

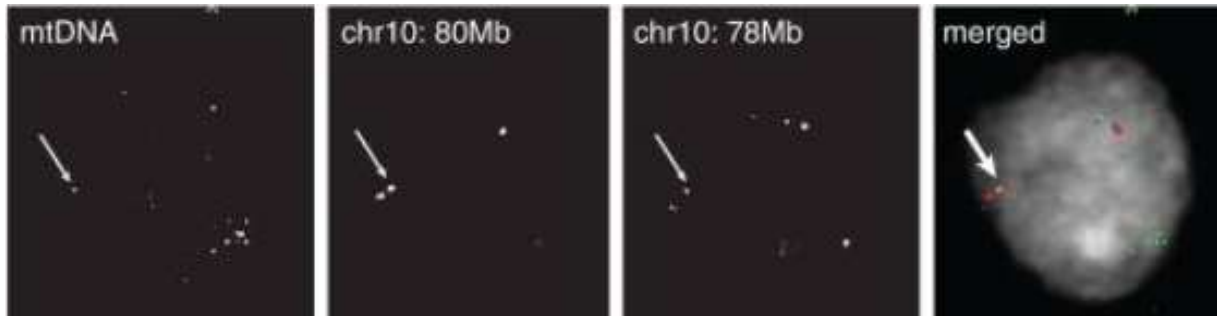Hazkani-Covo et al. PLoS Genet. 2010; 6(2):e1000834.

Mitochondrial-nuclear genome fusion sequences are present in cancer cells

Table 1. Summary of somatic mitochondrial-nuclear DNA fusions identified from 12 cancer samples

In **12 samples** (out of **587 samples**), 25 cancer-specific mitochondrial-nuclear DNA junctions were identified. **Breast cancer** (PD11372a) showed a somatically acquired **integration of almost the entire human mtDNA sequence** (**16,556 bp**) into chr.10q22.3.
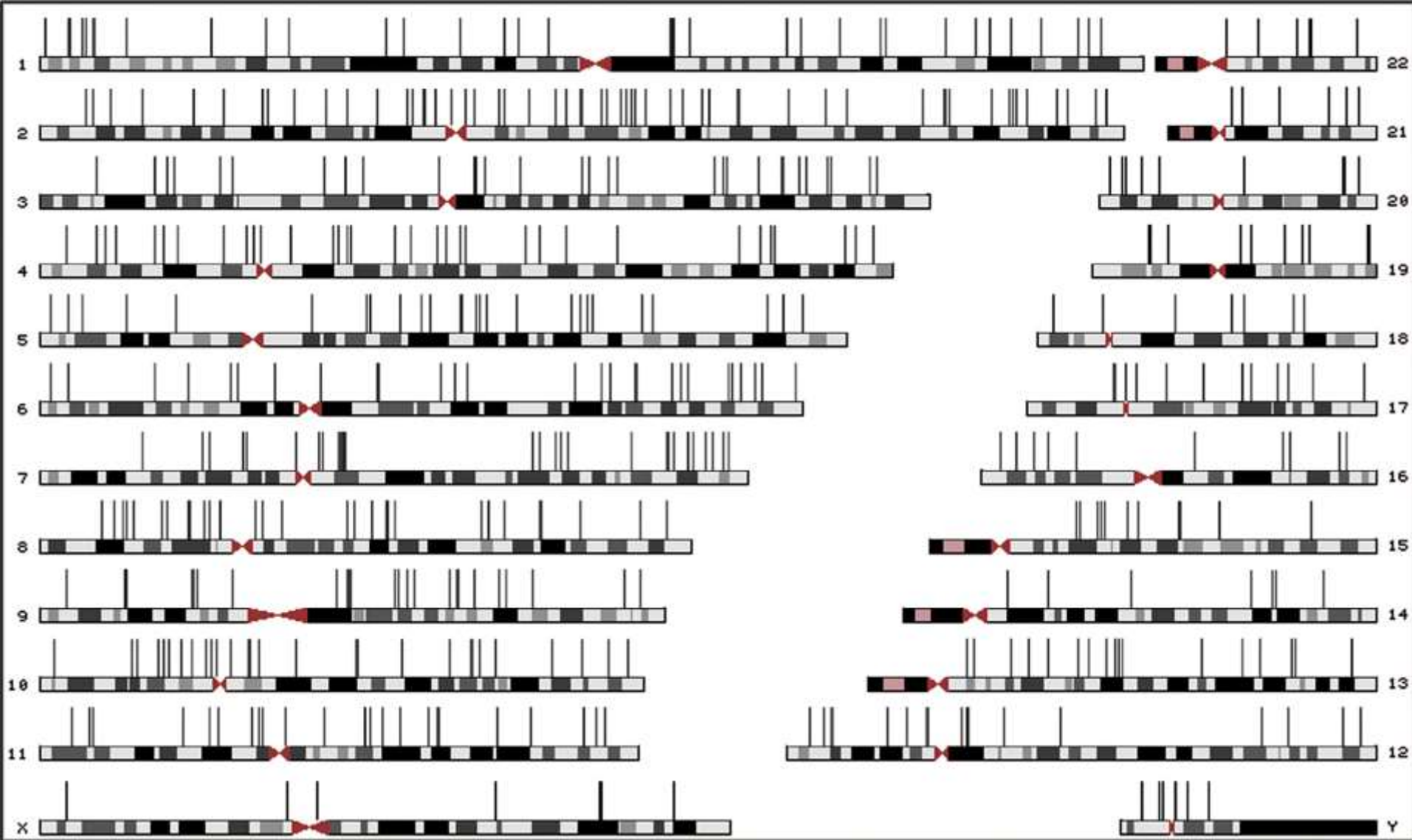
NUMTs (nuclear DNA sequences of mitochondrial origin) distribution in human chromosomes. Over 1600 NUMTs have been detected in the human genome.
Chromosome 2 and chromosome 18 are respectively the most and least densely populated by this class of genomic elements in terms of base pairs overall length.

- **Cell-free DNA** (or cfDNA) refers to all **non-encapsulated DNA** in the blood stream. Also **circulating extracellular nucleic acids**, including cell-free DNA (cfDNA), mRNA, and microRNA (miRNA)

- cfDNA are nucleic acid fragments that enter the bloodstream during apoptosis or necrosis. Normally, these fragments are cleaned up by macrophages, but the overproduction of cells in cancer leaves more of the cfDNA behind.

- These fragments average around **170 bases in length**, have a half-life of about two hours, and are present in both early and late stage disease in many common tumors including non-small cell lung and breastcfDNA concentration varies greatly, occurring at between 1 and 100,000 fragments per millilitres of plasma.

- **yme1 gene mutation cause the inactivation of YMe1p protein, a mitochondrial-localized ATP-dependent metalloprotease. That leads to high escape rate of mtDNA to the nucleus.**

- *OPA1* gene. This protein regulates mitochondrial fusion and cristae structure in the inner mitochondrial membrane and contributes to ATP synthesis and apoptosis,

Main influence of cfDNA
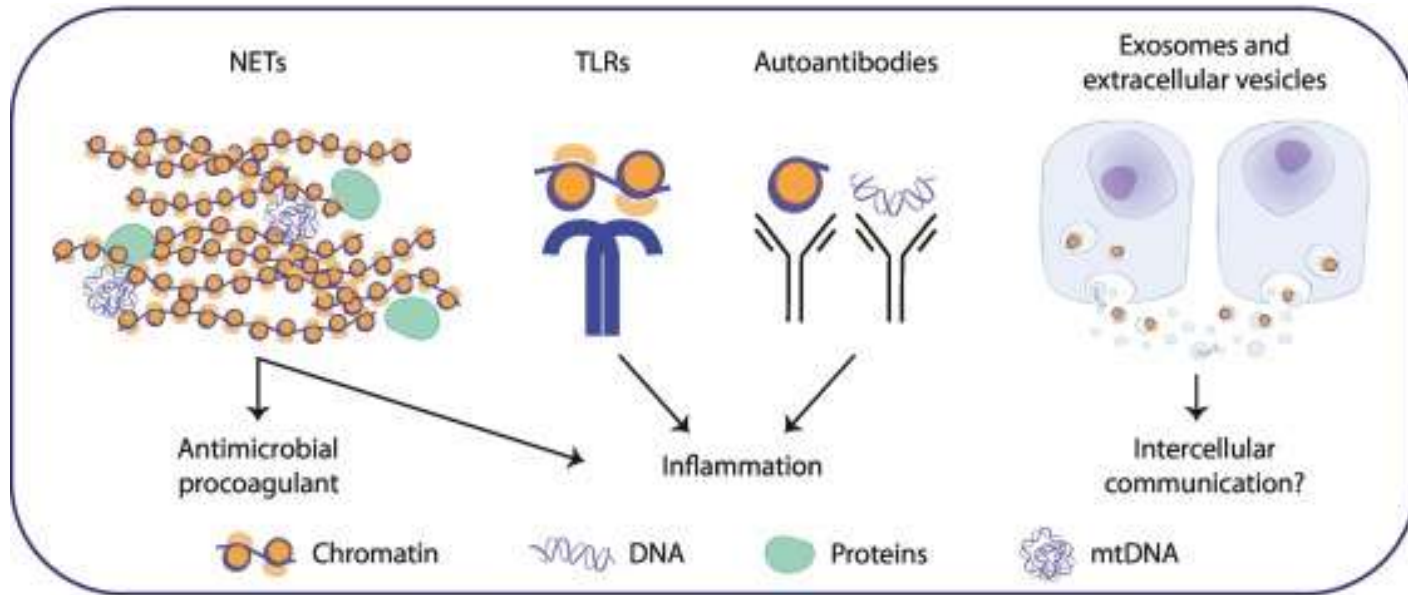
- **Immunomodulation and tumor-associated inflammation**. Extracellular **mtDNA** activates TLR9. AIM2 and NLRP3 inflammasomes induce the secretion of proinflammatory cytokines and initiate cytokine storm (e.g. **in COVID-19**).

- **Transforming ability** and functional **modulation of other cells**. Was demonstrated when NIH3T3 murine cells were treated with serum from patients with colon cancer. cfDNA was found in the murine chromosomes.

- **Tumor growth and metastatic niche establishment**. Can induce neutrophil extracellular traps (NETs) formation. NETs might influence the cancer microenvironment, promote tumor growth, and contribute to the establishment of a pre-metastatic niche.

Analysis of cell-free DNA in cells exposed to radiation using qPCR

Lack of a tool to predict **radiation therapy (RT) toxicity** is an important limitation in personalized care, as there are known variations in patients' normal tissue sensitivities to radiation. The QuantiDNA RadTox System (DiaCarta, Richmond, CA) is a patented technology (8,404,444: method for predicting the level of damage to cells by measuring free circulating *Arthrobacter luteus* (Alu nucleic acid) repetitive DNA sequences, which measures tissue damage shortly after RT exposure (Lockney et al., 2022). When most of the tissue exposure is normal tissue (not tumor), the circulating cell-free DNA (cfDNA) is **an indicator of normal tissue toxicity**; when most of the tissue exposure is treatment volume and tumor (such as with stereotactic ablative RT), it is an **indicator of tumor response** (Lockney et al., 2022). Thus, **cfDNA** can be considered as **novel biomarker** of radiation impact in humans.

Isolation of cell-free DNA

Cell-free DNAs (cfDNAs) are DNA fragments ranged between 50-1000 bp. cfDNA analysis can be performed using blood samples (serum or plasma), the main source of cfDNA, followed by urine, cerebrospinal fluid, pleural fluid, and cell culture medium samples.

Plasma or cell culture medium → **Binding** → **Washing: 1XWash Buffer1 1XWash Buffer2** → **Eluting** → **DNA Storage-20°C**

© Infographics · ZELLX®
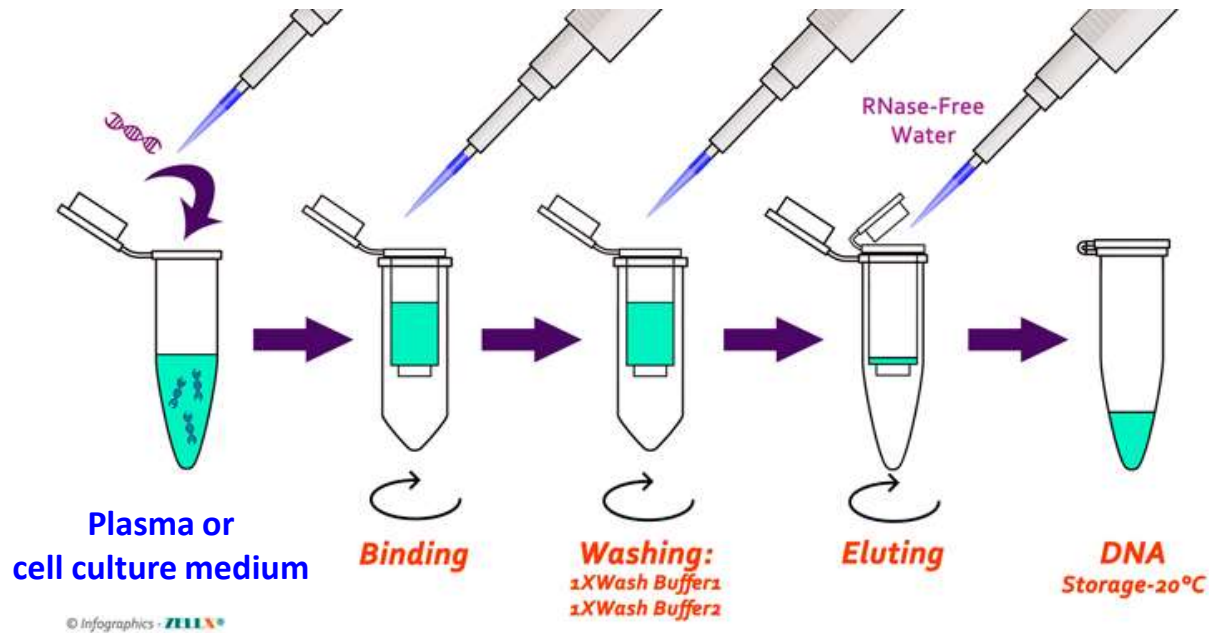
Analysis of cell-free DNA

cfDNA concentration can be measured by quantitative real-time PCR by comparing against the quantity of a human β-actin reference gene which is a one-copy gene.

Amplification Plot

Monocopy gene target
cfhDNA dtec-qPCR Test

ΔCt 6.00

Ct 25.96   Ct 31.96

ΔRn — Cycle
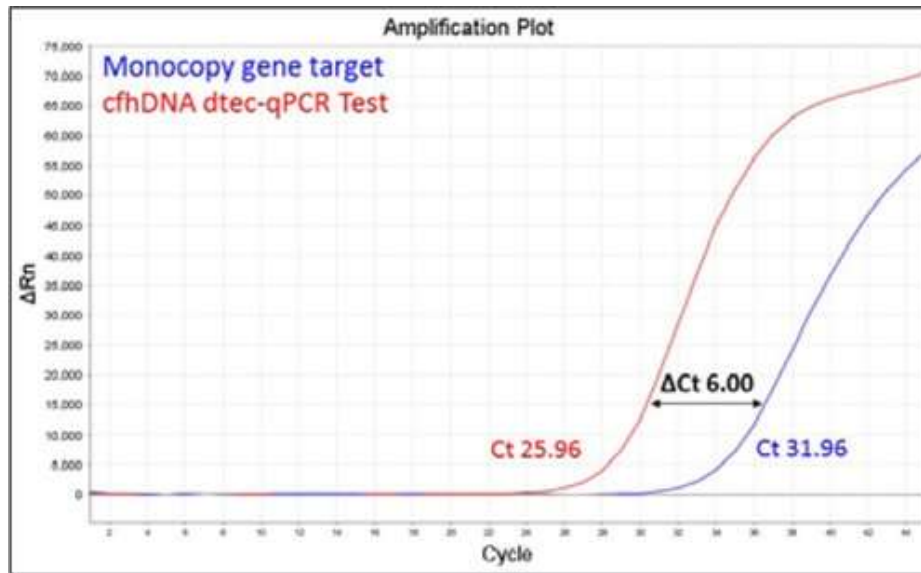
 Real-time PCR amplification plot for cfhDNA dtec-qPCR Test (red) targeting a "non-truncated" multi-copy gene and compared to a monocopy target (blue), using a human genomic DNA as a standard. Due to the presence of multiple copies of the selected target, sensibility is increased 2 logs (100 times) for the cfhDNA dtec-qPCR Test. Same increased signal is observed for the purified cell-free DNA samples employed for cell-free DNA quantification.

Applications of cfDNA analysis

Cisneros-Villanueva et al. Cell-free DNA analysis in current cancer clinical trials: a review. *Br J Cancer*. 2022;126(3):391-400.
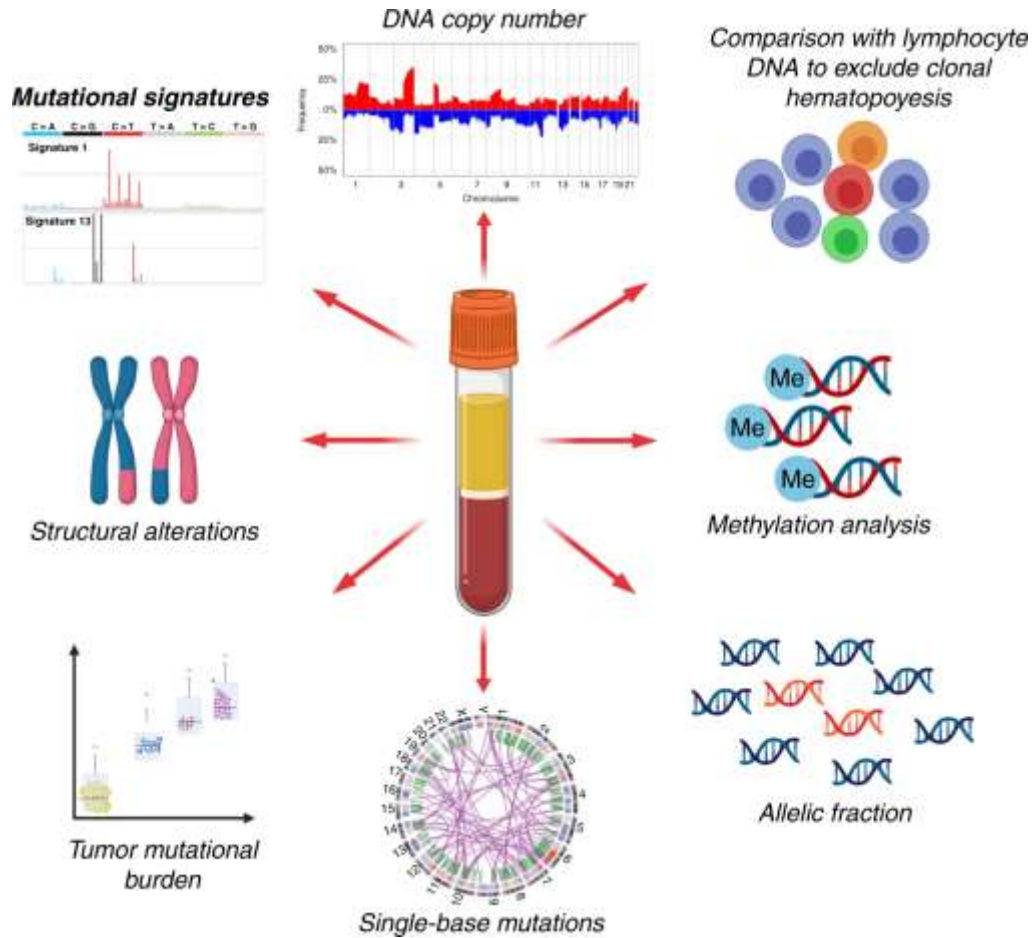
Extracellular vesicles

Extracellular vesicles (EVs) can be largely divided into three main subtypes: apoptotic bodies, microvesicles, and exosomes, and are classified based on their cellular origin, physiochemical, and biomolecular properties. The largest of these EVs, apoptotic bodies arise from the outward blebbing of an apoptotic cell membrane, resulting in phosphatidylserine-rich vesicles 500–5000 nm in diameter. Microvesicles originate as particles shedding from the plasma membrane and are enriched with phosphatidylserine and cholesterol, and typically are 100–1000 nm in diameter. **Exosomes are the smallest EVs** (30–150 nm) and are formed by the exocytosis of multivesicular bodies (MVBs) liberating intraluminal vesicles upon fusion with the plasma membrane.
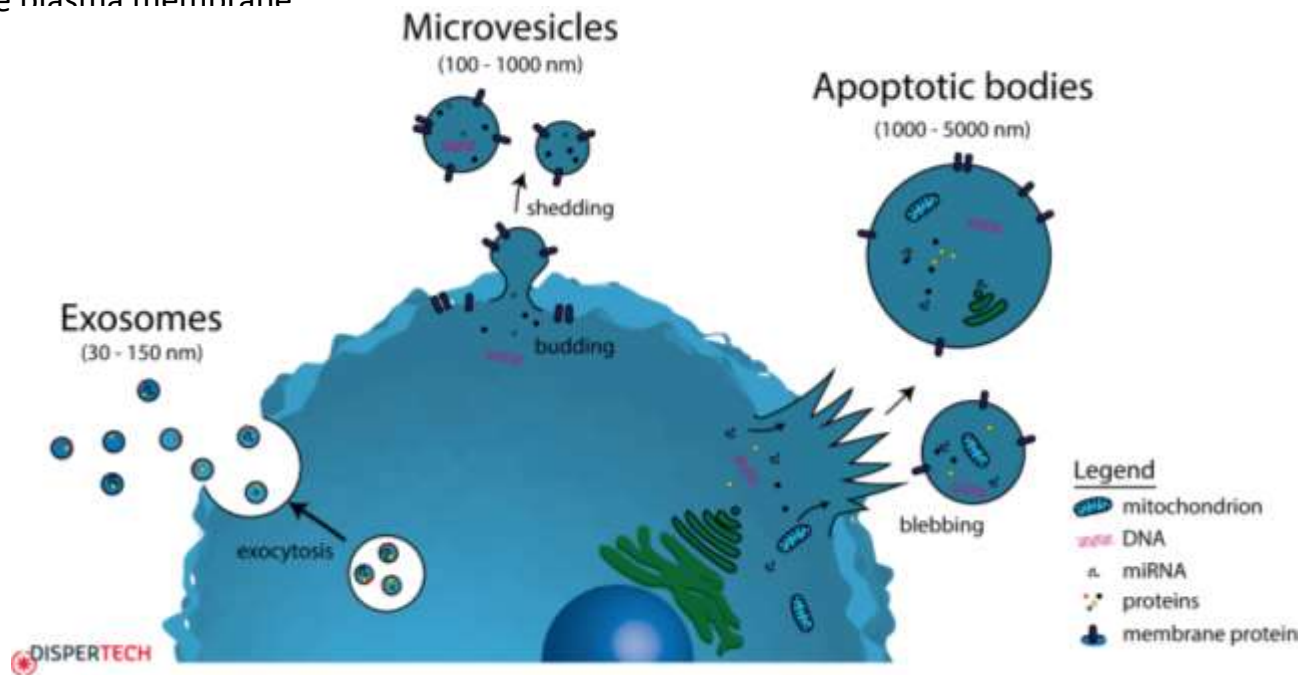
Isolation of EVs

"Capturem extracellular vesicle (EV) isolation kits" (Takara) are a complete solution for simple isolation of EVs in <30 min. These columns use a lectin-based binding compound to selectively isolate EVs from various biofluids. Ultracentrifugation is slow, damages EVs, and pulls down contaminants, confounding results. Other methods, like precipitation, are inconsistent, with low yield and purity. Our kits yield pure, intact EVs for downstream analyses, advancing diagnostic research and biomarker discovery.

Collecting supernatant

Pre-clear	Filter
2 min	10 min*

Isolating extracellular vesicles

Equilibrate	Bind	Wash	Elute
2 min	2 min	2 min	2 x 2 min

Transcriptomic analysis *Cell cultures* and cultivation conditions

H1299 (p53-deficient) and A549 (p53-wild-type) cell lines were obtained from the American Type Culture Collection (ATCC) and cultured in DMEM/F12 supplemented with 10% fetal bovine serum, 2.5 mM L-Glutamine,100 IU/mL penicillin, and 100 µg/mL streptomycin at 37 °C in 5% CO_2.

Irradiation

Conventional X-ray irradiation was performed using a 200 kV X-ray RUB RUST-M1 X-irradiator facility (JSC "Ruselectronics", Moscow, Russia). The exposure at a dose rate of 0.85 Gy/min (2.5 mA, 1.5 mm Al filter) at room temperature was applied to cells in logarithmic growth state. Ultrashort beam irradiation was carried out using an electron beam generated by a laser-driven radiofrequency gun-based linear AREAL accelerator (doi: 10.1016/j.nima.2016.02.028). The parameters of the AREAL laser-generated electron beam are presented in Table 1.

AREAL Beam Parameters		UV Laser Parameters	
Beam charge (pC)	30	Wavelength (nm)	258
Electron energy (MeV)	3.6	Pulse energy (µJ)	200
Pulse duration (fs)	450	Repetition rate (Hz)	1 – 50
Pulse repetition rate (Hz)	1 – 50	Energy stability	<1%
Beam spot size (mm)	15	Beam divergence (mrad)	<0.3
Norm. emittance (mm-mrad)	<0.5	Beam diameter (mm)	2.0
RMS energy spread	<1.5%	-	-
Online dose information	Faraday cup	-	-

Cells were irradiated at doses of 0.25–10 Gy (~140 electron pulses per 1 Gy) with a repetition rate of **20 Hz**. **A peak dose rate of 1.6×10^{10} Gy/s was estimated from the electron pulse duration of 4.5×10^{-13} s**, based on the laser pulse length, acceleration process, and electron beam transport. The mean absorbed **dose-rate of 11.70 ± 0.98 Gy/min** (repetition rate 20 Hz sample mass of 4.2 g) was calculated over the period of irradiation and 1% charge fluctuation and 1% beam energy fluctuation was taken into account.

Transcriptomic analysis

Exponentially growing A549 and H1299 cells were exposed to 2 Gy either of AREAL or X-rays.

RNA libraries were created, sequenced, and initially analyzed according to the protocols previously used to create the Atlas of RNA Sequencing Profiles of Normal Human Tissues. RNA isolation was performed using the QIAGEN RNeasy Kit (Qiagen), and the length of the isolated RNA (RIN) was measured using an Agilent 2100 bioanalyzer (Agilent, USA). RNA concentration was measured using a Qubit RNA Assay Kit. Ribosomal RNA was removed using the KAPA RNA Hyper Kit with RiboErase. Library concentrations and length distribution of amplified cDNA were measured using the Qubit dsDNA HS As-say kit and Agilent TapeStation (Agilent), respectively. Samples were sequenced using an **Illumina NextSeq 550** instrument using a **protocol for single-ended reads with an average length of 75 bp. with a reading depth of about 30 million per sample**. **Primary quality control of data from sequenced libraries was performed using the Illumina SAV software. Demultiplexing was performed using the Illumina Bcl2fastq2 v2.17 program according to the publication.**

Bioinformatics analysis

FASTQ read files were analyzed using the **STAR software [doi:10.1093/bioinformatics/bts635] in "GeneCounts" mode using transcriptome annotation from Ensembl (GRCh38 genome assembly and GRCh38.89 transcriptome annotation).** In total, **expression levels of 36596 genes were measured**. The data was normalized using DESeq2 [doi:10.1186/s13059-014-0550-8]. Changes in the activation of intracellular molecular pathways of irradiated cells compared to control cells were quantified using the Oncobox bioinformatics platform [doi:10.3390/cancers10100365].

Pathway activation level (PAL) for each molecular pathway was calculated using the formula:

$$PAL_p = \sum_n ARR_{np} \times \ln CNR_n \div \sum_n |ARR_n|, \qquad (10)$$

where PALp is the level of activation of the molecular pathway p; CNRn (case-to-normal ratio) - the ratio of gene n expression level in a tumor sample under study to an average level for the control group; ln is the natural logarithm; the discrete ARRnp value (role of activator/repressor) of gene n product in the p pathway is determined as follows: ARRnp is −1 if gene product n inhibits pathway p; 1 if n activates pathway p; 0 if n has ambiguous or unclear role in a pathway p; 0.5 or −0.5, if n is rather activator of a pathway or its inhibitor, respectively.

Statistics

Statistical and mathematical analyses of the data were conducted using the **Statistica 8.0 software** (StatSoft, Tulsa, OK, USA). The results are presented as the means of three independent experiments ± standard error. Statistical significance was tested using the Student t-test. The slope coefficients of dose–response curves were compared using the Z-test.

Babayan, N.; Vorobyeva, N.; Grigoryan, B.; Grekhova, A.; Pustovalova, M.; Rodneva, S.; Fedotov, Y.; Tsakanova, G.; Aroutiounian, R.; Osipov, A.

The aim of this work was to compare the formation and elimination of γH2AX and 53BP1 foci (well known markers for DNA double-strand breaks (DSBs)) in Hela cells exposed to ultrashort pulsed electron beams generated by Advanced Research Electron Accelerator Laboratory (AREAL) accelerator (electron energy 3.6 MeV, pulse duration 450 fs, pulse repetition rates 2 or 20 Hz) and quasi-continuous radiation generated by Varian accelerator (electron energy 4 MeV) at doses of 250–1000 mGy.

Colony–Forming Ability and Residual Foci of DNA Repair Proteins in Human Lung Fibroblasts Irradiated with Subpicosecond Beams of Accelerated Electrons

N S Babayan [1] [2], D V Guryev [3] [4], N Yu Vorobyeva [3] [4], B A Grigoryan [5], G L Tadevosyan [1], L S Apresyan [1], A K Chigasova [3] [6], E I Yashkina [4], S M Rodneva [4], A A Tsishnatti [4], Yu A Fedotov [3] [4], N K Sarkisyan [1], A T Manukyan [2], R M Aroutiounian [2], A N Osipov [7] [8]

Affiliations + expand

We performed a comparative study of the colony-forming ability and the number of residual foci of DNA repair proteins in cultured **human lung fibroblasts (MRC-5 cell line)** after exposure to subpicosecond beams of accelerated electrons with an energy of 3.6 MeV and quasi-continuous radiation (accelerated electrons with an energy of 4 MeV and X-rays). **The yield of damages causing reproductive cell death after pulsed subpicosecond radiation exposure was higher by ~1.8 times than after quasi-continuous radiation exposure.**

The quantitative yield of **residual γH2AX foci in irradiated cells was shown to be ~2.0-2.5-fold higher than in cells irradiated with quasi-continuous beams of accelerated electrons.**